



**HAL**  
open science

**Palaeomagnetism and K-Ar and  $^{40}\text{Ar}/^{39}\text{Ar}$  ages in the Ali Sabieh area (Republic of Djibouti and Ethiopia): constraints on the mechanism of Aden ridge propagation into southeastern Afar during the last 10 Myr**

L. Audin, X. Quidelleur, E. Coulié, V. Courtillot, S. Gilder, I. Manighetti, P. -Y. Gillot, P. Tapponnier, T. Kidane

► **To cite this version:**

L. Audin, X. Quidelleur, E. Coulié, V. Courtillot, S. Gilder, et al.. Palaeomagnetism and K-Ar and  $^{40}\text{Ar}/^{39}\text{Ar}$  ages in the Ali Sabieh area (Republic of Djibouti and Ethiopia): constraints on the mechanism of Aden ridge propagation into southeastern Afar during the last 10 Myr. *Geophysical Journal International*, 2004, 158, pp.327-345. 10.1111/j.1365-246X.2004.02286.x . insu-03600280

**HAL Id: insu-03600280**

**<https://insu.hal.science/insu-03600280>**

Submitted on 7 Mar 2022

**HAL** is a multi-disciplinary open access archive for the deposit and dissemination of scientific research documents, whether they are published or not. The documents may come from teaching and research institutions in France or abroad, or from public or private research centers.

L'archive ouverte pluridisciplinaire **HAL**, est destinée au dépôt et à la diffusion de documents scientifiques de niveau recherche, publiés ou non, émanant des établissements d'enseignement et de recherche français ou étrangers, des laboratoires publics ou privés.



Distributed under a Creative Commons Attribution 4.0 International License

# Palaeomagnetism and K-Ar and $^{40}\text{Ar}/^{39}\text{Ar}$ ages in the Ali Sabieh area (Republic of Djibouti and Ethiopia): constraints on the mechanism of Aden ridge propagation into southeastern Afar during the last 10 Myr

L. Audin,<sup>1,2,\*†</sup> X. Quidelleur,<sup>1,3</sup> E. Coulié,<sup>3</sup> V. Courtillot,<sup>1</sup> S. Gilder,<sup>1</sup> and I. Manighetti,<sup>2</sup>  
P.-Y. Gillot,<sup>3</sup> P. Tapponnier<sup>2</sup> and T. Kidane<sup>4</sup>

<sup>1</sup>Laboratoires de Paléomagnétisme, Institut de Physique du Globe de Paris, 75230 Paris Cedex 05, France

<sup>2</sup>Laboratoires de Tectonique, Institut de Physique du Globe de Paris, 75230 Paris Cedex 05, France

<sup>3</sup>Laboratoire de Géochronologie Multi-Techniques UPS-IPGP, Bat. 504 Sciences de la Terre, Université Paris-Sud, 91405 Orsay, France

<sup>4</sup>Department Of Geology and Geophysics, University of Addis-Ababa, Ethiopia

Accepted 2004 February 24. Received 2004 February 24; in original form 2002 November 25

## SUMMARY

A new detailed palaeomagnetic study of Tertiary volcanics, including extensive K-Ar and  $^{40}\text{Ar}/^{39}\text{Ar}$  dating, helps constrain the deformation mechanisms related to the opening processes of the Afar depression (Ethiopia and Djibouti). Much of the Afar depression is bounded by 30 Myr old flood basalts and floored by the *ca* 2 Myr old Stratoid basalts, and evidence for pre-2 Ma deformation processes is accessible only on its borders. K-Ar and  $^{40}\text{Ar}/^{39}\text{Ar}$  dating of several mineral phases from rhyolitic samples from the Ali Sabieh block shows indistinguishable ages around 20 Myr. These ages can be linked to separation of this block in relation to continental breakup. Different amounts of rotation are found to the north and south of the Holhol fault zone, which cuts across the northern part of the Ali Sabieh block. The southern domain did not record any rotation for the last 8 Myr, whereas the northern domain experienced approximately  $12 \pm 9^\circ$  of clockwise rotation. We propose to link this rotation to the counter-clockwise rotation observed in the Danakil block since 7 Ma. This provides new constraints on the early phases of rifting and opening of the southern Afar depression in connection with the propagation of the Aden ridge. A kinematic model of propagation and transfer of extension within southern Afar is proposed, with particular emphasis on the previously poorly-known period from 10 to 4 Ma.

**Key words:** geochronology, paleomagnetism, plate boundary, rifted margin.

## 1 INTRODUCTION

Understanding the relative timing and spatial distribution of volcanism and continental rifting should provide important constraints on the mechanics of continental breakup (Courtillot *et al.* 1999). The Afar depression, a triple-plate junction located in a hotspot area, is recognized as a unique setting to study these mechanisms (Fig. 1). Since 30 Ma, the Ethiopian plume head has influenced a vast area centered on the present day Afar depression (Hofmann *et al.* 1997; Coulié *et al.* 2003). When both the Aden and Red sea propagators (Fig. 2a) arrived near the junction area (*ca* 20 Ma; Courtillot

*et al.* 1987), the Afar depression started to open. It seems that two continental microplates, the Danakil and Ali Sabieh blocks, were isolated and that the depression started to stretch as these blocks began rotating (Fig. 2a; Audin 1999). The Danakil block rotated counter-clockwise by  $10.7 \pm 4^\circ$  with respect to stable Africa in the last 7 Myr (Fig. 2a; Manighetti *et al.* 2001). Prior to the present study, no data existed for the Ali Sabieh area, which mirrors the Danakil block south of the gulf of Tadjoura. Moreover, because the depression is floored by the *ca* 2 Myr old Stratoid basalts, older deformation events are masked within central Afar.

For the last 2 Myr, the central Afar has been dominated by a bookshelf faulting tectonic regime (Fig. 1; Tapponnier *et al.* 1990). Since approximately 1 Ma, the Aden rift has moved inland along the western edge of the Danakil block and has propagated northwards (Fig. 1). At the same time, the southern termination of the Red Sea ridge system, already established at the Manda-Hararo rift

\*Corresponding author: IPGP/Laboratoire de Tectonique et de Paléomagnétisme, 4 place Jussieu, 75252 Paris cedex 05, France.

†Now at: IRD-Univ. P. Sabatier, Géologie, 38 rue des 36 ponts, 31400 Toulouse, France. E-mail: Laurence.Audin@ird.fr

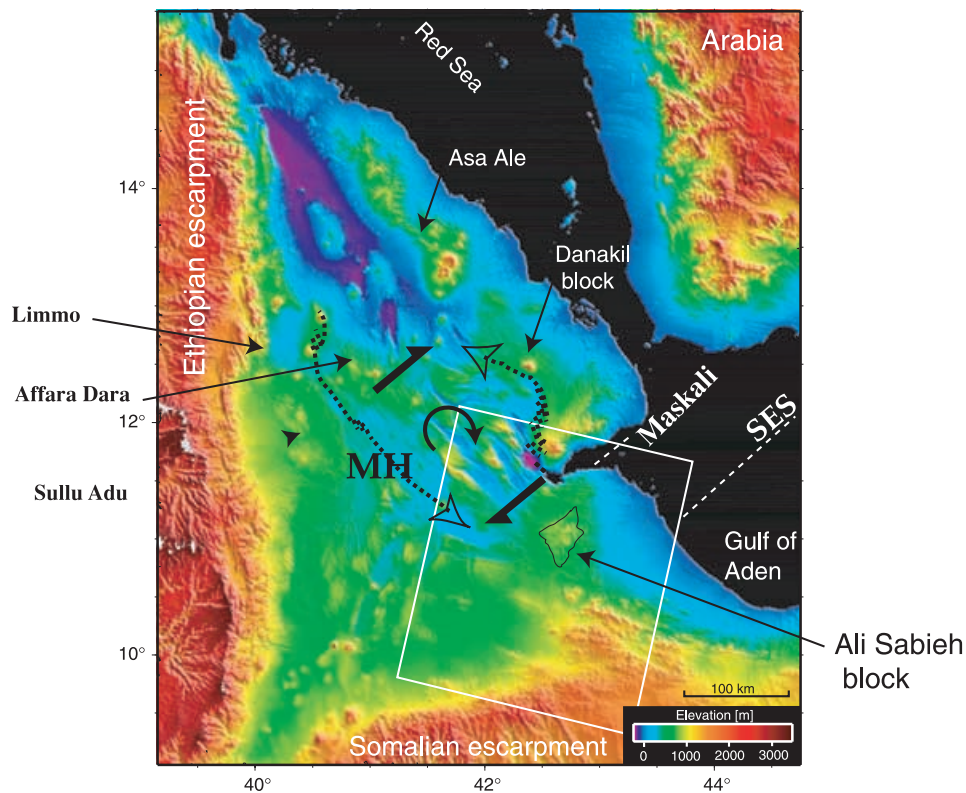


**Figure 1.** General location of the study area (white rectangle between the tip of the Aden Gulf and the Somalian escarpment). The Danakil and Ali Sabieh blocks show higher altitudes than the rest of the depression on this topographic map. Rift segments inland are shown as thick dashed lines. Thick black arrows outline shear on the overlap zone of bookshelf faulting (Tapponnier *et al.* 1990). Shukra el Sheik discontinuity (SES); Manda Hararo rift zone (MH).

(Fig. 1), propagated southwards along the western edge of the Afar depression, which is now the Ethiopian escarpment (e.g. Lahitte *et al.* 2003). In the process, a large overlap was formed (Fig. 1; Courtillot *et al.* 1984; Manighetti *et al.* 2001; Kidane *et al.* 2003).

The mechanism governing the opening of the Afar depression between 20 and 1 Ma is not well documented. Some form of saloon doors opening is suspected to have been the initial crustal process related to penetration of the Aden ridge in the Afar continental area (Fig. 2a; Manighetti *et al.* 1998). In the present study, we have focused our palaeomagnetic and geochronological investigations in the Ali Sabieh area, where the oldest outcrops in Afar have been identified (from 20 to 1 Ma, Figs 2b and 3). New K/Ar determinations obtained around the Ali Sabieh block help to constrain the ages of the various formations. The purpose of this new regional study is to define the geometry and chronology of the tectonic phases that characterize continental breakup of East Africa and the opening of the Afar depression (Fig. 2).

## 2 THE ALI SABIEH REGION

### 2.1 Geological framework

The Ethiopian traps constitute the oldest volcanic markers of Afar breakup and are found on its western and southern topographic margins (Figs 1 and 2). A combination of  $^{40}\text{Ar}/^{39}\text{Ar}$  ages and palaeomagnetic results (Hofmann *et al.* 1997; Rochette *et al.* 1998) have shown that these traps erupted approximately  $30 \pm 1$  Ma in a very short time-span. Recent K-Ar and  $^{40}\text{Ar}/^{39}\text{Ar}$  determinations have confirmed the coeval emplacement of both the Ethiopian and Yemenite traps, with a duration significantly less than 1 Myr for most of the

basaltic pile (Coulié *et al.* 2003). Some 26 Myr later, the Stratoid series flooded the whole surface of the depression. This thick basaltic formation erupted during the last 4 Myr with a south to north volcanic migration (Lahitte *et al.* 2002). Because the Stratoid basalts represent an excellent marker of the recent deformation, they have been extensively studied (Figs 1 and 3).

In contrast, the Ali Sabieh area on the edge of the depression has remained geologically and tectonically poorly explored. Only a few publications, mostly related to geological mapping of Afar, describe the tectonic setting of the area (Beydoun 1970; Black *et al.* 1975; Chessex *et al.* 1975; Muller & Boucarut 1975; Gaulier & Huchon 1991). The Ali Sabieh block lies at approximately 1300 m elevation, which has led some authors to identify this area as a tectonic horst. Because no evidence for uplift can be observed, we prefer to define it as a block (Figs 2 and 3). Thanks to its characteristic triangular shape, the Ali Sabieh area can be easily distinguished either on topographic or geological maps (Figs 2 and 3). Its central part mainly consists of a Precambrian sedimentary basement, which only outcrops in the Ali Sabieh region (Fig. 3). It consists of metamorphic series and is covered in some places by Jurassic limestones and continental sandstones of lower Cretaceous age (Varet & Gasse 1978).

The oldest volcanic formations identified within Afar, the Adolei basalts, were emplaced during the Oligocene–Miocene, from 27 to 20 Ma (Table 1). They are mainly associated with dykes with variable orientations that intrude the sedimentary basement and are sometimes located on the edges of the sedimentary core of the block (Black *et al.* 1975). In order to avoid any confusion with the Mabl series, also present in the Adolei area, we chose to rename the products from the Adolei basaltic event as Old basalt:  $\beta_0$  (Fig. 2). These basalts may be contemporaneous (22–18 Ma) with other volcanic

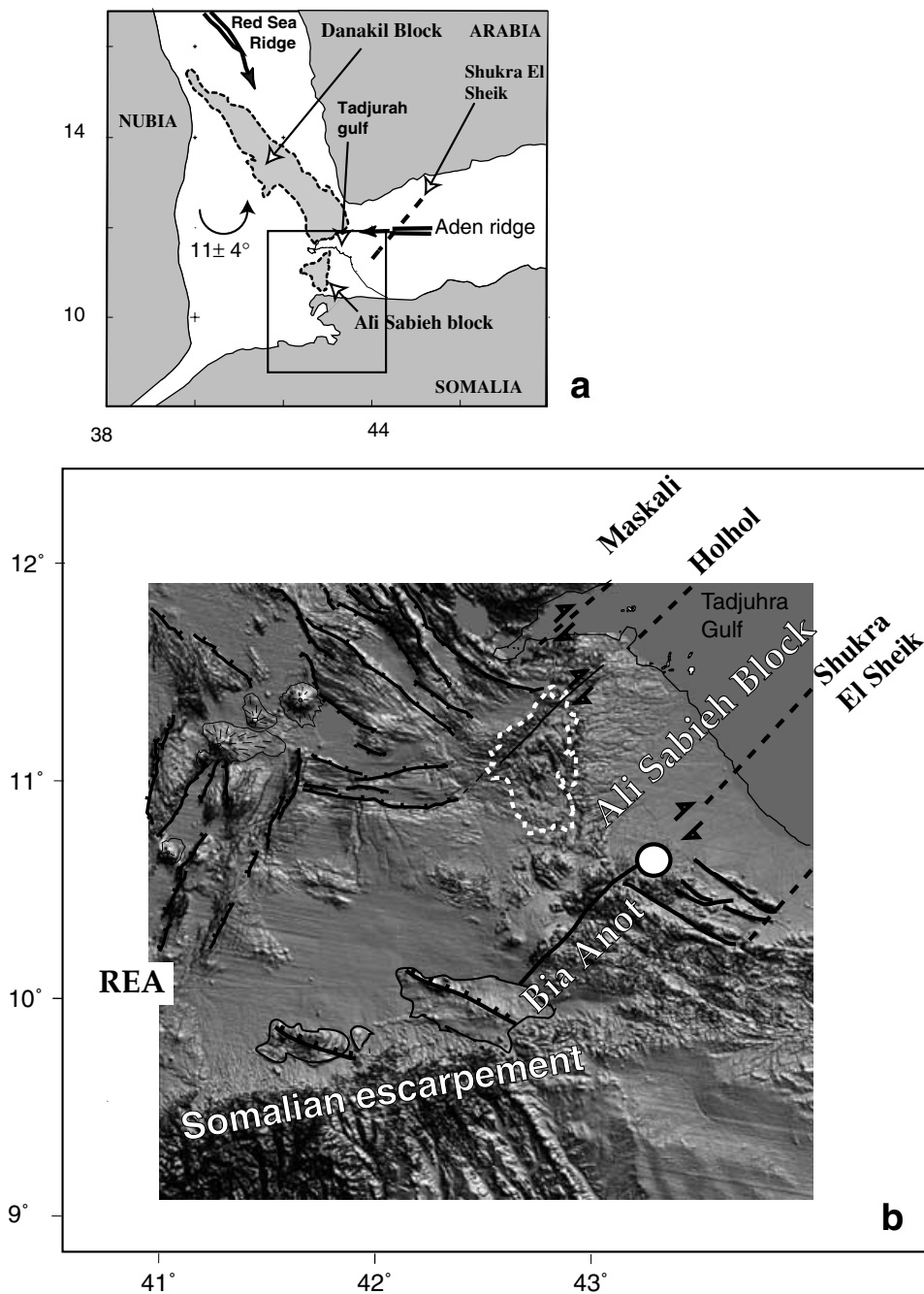


**Figure 2.** (a) Outlines of the Danakil and Ali Sabieh blocks. Amount of counter-clockwise rotation of the Danakil block after Manighetti *et al.* (2001). (b) Topographic Digital Elevation Model (DEM; Gupta & Scholz 2000) and tectonic framework (this study) of the Ali Sabieh. Main faults in central Afar are from this study and Manighetti *et al.* (2001), and Kidane *et al.* (2003). East African rift (EAR). The location of the 1980 seismic crisis is reported as a large white dot (Ruegg *et al.* 1981). Outline of the Ali Sabieh block is dashed. The newly defined Young volcanic lava fields along the Somalian escarpment are also shown (see text).

series found on the Ethiopian plateau (Baker *et al.* 1996; Rochette *et al.* 1998). During this time interval, granitic intrusions have been reported in the southern part of the Ali Sabieh block (22–18 Ma; Fig. 2; Chessex *et al.* 1975). Because peralkaline granites are generally associated with the initial stages of continental breakup, they could be considered to be the first magmatic event clearly related to the initiation of continental rifting. A few other granitic bodies, dated between 26 and 22 Ma by conventional K-Ar, are reported elsewhere in Afar: at the northern end of the Sullu Adu massif, within the Limmo massif, in Affara Dara (central Afar) and at the

southern termination of the Danakil block (Fig. 1; Varet & Gasse 1978). Using the  $^{40}\text{Ar}/^{39}\text{Ar}$  isochron approach to correct for a non-atmospheric Ar component, Coulié (2001) has shown that these granites were actually intruded approximately 30 Ma, coeval with trap emplacement.

The Ali Sabieh basement is also surrounded and intruded by a younger succession of rhyolitic dykes and basaltic lava flows, which are also found south of the Danakil block. The oldest phase of this group, mainly composed of rhyolites, corresponds to the Mabla series, while the youngest, called the Dahla series, consists of basaltic

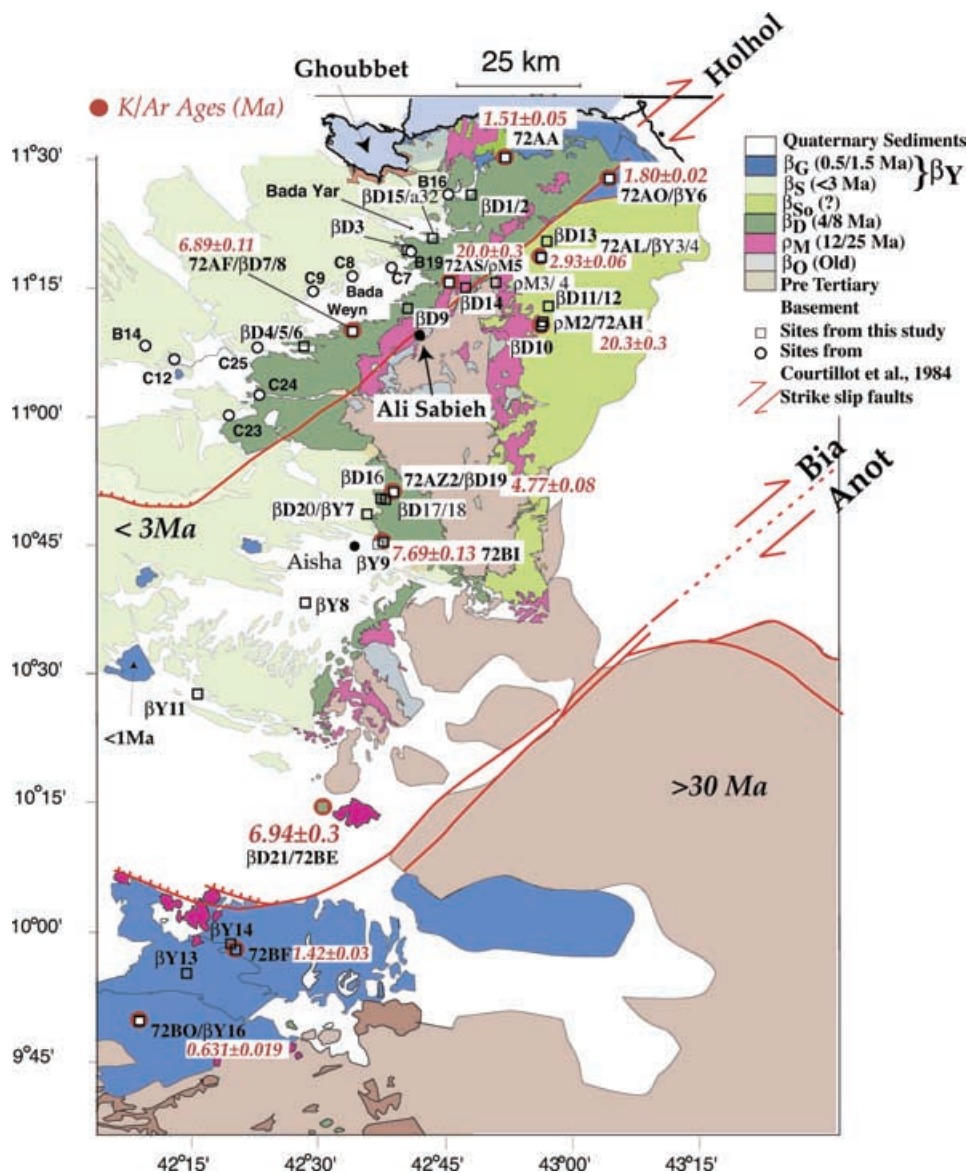


**Figure 3.** Detailed geological map of the Ali Sabieh area, modified from Varet & Gasse (1978). Sites with palaeomagnetic and K/Ar data are reported with their codes (squares for this study and circles from Courtyllo *et al.* 1984). Age determinations from this study are shown next to the appropriate sites. Main faults are indicated, notably the Bia Anot and Holhol fault systems. Towns are shown as full black circles.

products (Fig. 3). The Mabla series ( $\rho M$ ) was emplaced from 25 to 12 Ma around the Ali Sabieh block and consists of rhyolitic dykes, domes, some ignimbrite layers and basaltic lava flows (Varet & Gasse 1978; Zumbo *et al.* 1995) (Table 1; Fig. 3). These rocks are commonly altered by fluid circulation. The Mabla formation surrounds the triangular shape of the pre-Tertiary basement on its western and eastern borders to the north (Fig. 3). Rhyolitic volcanism probably lasted almost 13 Myr south of the Gulf of Tadjoura, whereas it seemed to be younger and shorter in the Danakil block, north of the Gulf of Tadjoura. Based on photographic interpretations and on the few K/Ar ages available north of the Gulf of Tadjoura at that time, a correlation between those two rhyolitic series, north and south of the Gulf of Tadjoura was first proposed by Varet & Gasse (1978). However, it requires dating south of the Gulf of Tadjoura before it can be validated. In both regions, the Mabla rhyolitic phase was followed by the basaltic Dahla series. It has been shown in the Ali Sabieh area that a phase of erosion affected the Mabla forma-

tion before emplacement of the Dahla basalts (Varet & Gasse 1978). The latter formation, which consists of thick series of subhorizontal flows, crops out in the Danakil block, in the Ali Sabieh area and also in the Sullu Adu region at the base of the Ethiopian escarpment (Fig. 1). These basalts were dated by conventional K-Ar analyses between 8.3 and 4.3 Ma and are correlative with the Somali basalts ( $\beta So$ ), which were emplaced approximately during the same period of time (7.2–3 Ma): (Varet & Gasse 1978). The Dahla formation surrounds Ali Sabieh to its NW and SW, whereas the Somali basalts are found on the eastern side of Ali Sabieh (Fig. 3).

The most important volcanic formation in central Afar, both in volume and surface area, is the 1-km-thick basaltic Stratoid formation ( $\beta S$ ), is not found within the Ali Sabieh block (Fig. 3). The  $\beta S$  formation is mostly younger than 3.5 Myr in its major part (Courtyllo *et al.* 1984; Kidane *et al.* 2003; Lahitte *et al.* 2001). It borders and overlaps the older volcanic series on the western side of the Ali Sabieh block but is not identified on its eastern side (Fig. 3). The

**Table 1.** Previously published K/Ar and Ar/Ar ages in the Ali Sabieh region (Ar/Ar: plateau ages).

Sample number	Geological formations	Mineral phases	References	Ages (Myr)
JM41	$\beta A$	Whole rock	Chessex <i>et al.</i> (1975)	26.7 $\pm$ 1.0
GE11	$\beta A$	Whole rock	Chessex <i>et al.</i> (1975)	22.6 $\pm$ 0.9
W172	$\beta A$	Whole rock	Barberi <i>et al.</i> (1975)	20.0 $\pm$ 0.6
PP728	$\beta A$	Whole rock, Ar/Ar	Zumbo <i>et al.</i> (1995)	23.6 $\pm$ 0.5
RC11	$\rho M$	Whole rock	Chessex <i>et al.</i> (1975)	25.2 $\pm$ 0.9
93B	$\rho M$	Whole rock	Gasse & Varet (1986)	20.6 $\pm$ 2.0
PP718	$\beta M$	Plagioclase, Ar/Ar	Zumbo <i>et al.</i> (1995)	19.0 $\pm$ 0.3
MB263	$\rho M$	Whole rock	Gasse & Varet (1986)	18.8 $\pm$ 1.4
PP762	$\beta M$	Whole rock, Ar/Ar	Zumbo <i>et al.</i> (1995)	17.3 $\pm$ 0.2
PP765	$\rho M$	Whole rock, Ar/Ar	Zumbo <i>et al.</i> (1995)	16.7 $\pm$ 0.4
RC13	$\rho M$	Glass	Chessex <i>et al.</i> (1975)	13.3 $\pm$ 0.6
83L	$\rho M$	Perlite	Gasse & Varet (1986)	12.4 $\pm$ 0.5
80D	$\beta D$	Whole rock	Gasse & Varet (1986)	8.3 $\pm$ 0.6
W19	$\beta D$	Whole rock	Barberi <i>et al.</i> (1975)	8.0 $\pm$ 0.4
GE4	$\beta D$	Whole rock	Chessex <i>et al.</i> (1975)	7.9 $\pm$ 0.4
TF783	$\beta D$	Whole rock	Richard (1979)	5.9 $\pm$ 0.5
H448	$\beta D$	Whole rock	Barberi <i>et al.</i> (1975)	4.3 $\pm$ 0.2
TF740	$\beta D$	Whole rock	Richard (1979)	3.9 $\pm$ 0.4
MAS95	$\beta So$	Whole rock	Gasse & Varet (1986)	7.2 $\pm$ 1.4
X	$\beta So$	Whole rock	Chessex <i>et al.</i> (1975)	6.3 $\pm$ 1.2
DJ56	$\beta So$	Whole rock	Chessex <i>et al.</i> (1975)	5.0 $\pm$ 0.9
MAS92	$\beta So$	Whole rock	Gasse & Varet (1986)	3.0 $\pm$ 0.6
80C	$\beta S$	Whole rock	Gasse & Varet (1986)	3.1 $\pm$ 0.6
125.2	$\beta S$	Whole rock	Courtillot <i>et al.</i> (1984)	3.0 $\pm$ 1.4
TF633	$\beta S$	Whole rock	Richard (1979)	3.3 $\pm$ 0.3
TF736	$\beta S$	Whole rock	Richard (1979)	2.0 $\pm$ 0.2
52	$\beta S$	Whole rock	Gasse & Varet (1986)	0.8 $\pm$ 0.1
B1	$\beta S$	Whole rock	Courtillot <i>et al.</i> (1984)	0.7 $\pm$ 0.5
TF746	$\beta I$	Whole rock	Richard (1979)	2.8 $\pm$ 0.3
TF914	$\beta I$	Whole rock	Richard (1979)	1.0 $\pm$ 0.1

Gulf Basalt formation ( $\beta_G$ ) crops out in the northernmost part of the Ali Sabieh block, on the border of the Gulf of Tadjoura. This series was emplaced during the first stages of rifting along the proto-Gulf of Tadjoura (Richard 1979). Each of these basaltic formations can be distinguished on the field and moreover presents a different geochemical signature in the laboratory (Varet & Gasse 1978).

## 2.2 Tectonic framework

The boundary between central Afar and the Ali Sabieh region is marked by a NE trending string of small en-échelon sedimentary basins, which are not bounded by NE striking faults (Bada Weyn and Bada Yar; Figs 1 to 3). Major NW–SE trending normal faults are described in central Afar (Tapponnier *et al.* 1990), while the northwestern edge of the Ali Sabieh block is cut by a dense network of minor EW trending normal faults. These tectonic features, mainly present in the Dahla formation, do not cut the Holocene sediments that fill the small basins and seem to veer from the Stratoid central series into the Dahla series (Figs 2 and 3). These presently inactive tectonic features seem to root in the pre-Tertiary basement (Fig. 3).

Analyses of SPOT images reveal the presence of large inactive NE–SW strike-slip faults cutting through the Ali Sabieh region (Black *et al.* 1975). This trend coincides with the present-day transform fault trend of the eastern Gulf of Aden (Tamsett & Searle 1990). Two major such fault systems appear to trend parallel to the NE striking alignment of the small sub-basins (Bada Weyn and Bada Yar; Fig. 3): the Holhol fault system, which crosses the Ali Sabieh block to the north, and the Bia Anot fault to the south (Black *et al.*

1975). Although the Bia Anot fault does not show clear evidence for recent activity south of the basement outcrop, it was apparently associated with a seismic event in 1980, with a 5.3 magnitude main shock (Ruegg *et al.* 1981). This sequence and aftershock seismicity define a 20°NW strike-slip mechanism (large open dot on Fig. 2). The two main NE trending tectonic systems are defined by major linear fault traces associated with smaller features trending in the same direction. These major strike slip features allow us to define three domains within the Ali Sabieh region, each being delimited by one or two NE–SW trending faults. Because no palaeomagnetic data have been obtained south of the Bia Anot fault, only two domains (delimited by the Holhol fault) are considered below.

The NE direction is also associated with the extension of the Mabla rhyolites in the northern part of the Ali Sabieh block towards the Gulf of Tadjoura, but no fault trace can be identified in the field or on satellite images (Figs 2 and 3). Similarly, the thick Stratoid formation is not cut by any NE trending faults, but it is cut by a dense NW–SE fault network that extends all over central Afar. This is particularly striking in Figs 1 and 2.

According to previous palaeomagnetic studies (Schult 1974; Galibert *et al.* 1980; Manighetti *et al.* 2001), the Danakil block underwent a 11  $\pm$  4° counter-clockwise rotation 7 Ma. These authors proposed that both this rotation and an assumed clockwise rotation of the Ali Sabieh block was linked to the opening of the Gulf of Tadjoura. It covers a shorter time range because it is based on samples ranging between 7 to 4 Ma around the Danakil block. As a matter of fact, the Maskali transform fault, in the Gulf of Tadjoura, displays the same NW–SE trend between the Danakil and Ali Sabieh blocks and shows some recent seismic activity (Figs 1 and

**Table 2a.** K-Ar results for basaltic samples. Column headings indicate: Sample (identification), K per cent (potassium concentration), per cent  $^{40}\text{Ar}^*$  (concentration of radiogenic  $^{40}\text{Ar}$ ),  $^{40}\text{Ar}^*$ (at./g; number of atoms of radiogenic  $^{40}\text{Ar}$  per gram), age (in Myr), Un. (uncertainty, in Myr). For each site, weighted mean age and uncertainty are also indicated, site (palaeomagnetic site name), polarities (T: transitionnal, N: normal, R: reverse). Not determined (n.d.)

Sample	K per cent	per cent $^{40}\text{Ar}^*$	$^{40}\text{Ar}^*$ (at./g)	Age (Myr)	Un. (Myr)	Formation	Site/Polarity
72BO	0.743	4.49 per cent	4.95837E + 11	0.639	0.023		
		7.09 per cent	4.85884E + 11	0.626	0.016		
				0.631	0.019		
72BF	0.901	7.23 per cent	1.35991E + 12	1.44	0.03	$\beta\text{Y}$	$\beta\text{Y}16 / \text{N}$
		8.71 per cent	1.31972E + 12	1.40	0.03		
				1.42	0.03		
72AA	0.378	4.97 per cent	6.01077E + 11	1.52	0.05		R
		5.00 per cent	5.91E + 11	1.50	0.05		
				1.51	0.05		
72AO	0.606	19.20 per cent	1.11096E + 12	1.75	0.02		n.d.
		25.95 per cent	1.16582E + 12	1.84	0.02		
				1.80	0.02		
72AL	0.740	7.786 per cent	2.062E + 12	2.67	0.06	$\beta\text{Y}$	$\beta\text{Y}6/\text{N}$
72AL1	0.400	4.95 per cent	1.099E + 12	2.92	0.09	$\beta\text{So}$	n.d.
72AL2	0.600	6.24 per cent	1.800E + 12	2.93	0.08	$\beta\text{So}$	$\beta\text{Y}2/\text{T}$
72AZ2	0.584	15.29 per cent	2.83231E + 12	4.64	0.08		$\beta\text{Y}3/\text{N}$
		21.09 per cent	2.97379E + 12	4.87	0.08		
				4.77	0.08		
72AF	0.375	13.75 per cent	2.70755E + 12	6.90	0.11	$\beta\text{D}$	$\beta 19/\text{R}$
		10.75 per cent	2.70172E + 12	6.88	0.12		
				6.89	0.11		
72BE	0.400	4.10 per cent	2.92361E + 12	6.98	0.27	$\beta\text{D}$	$\beta 7/\text{N}$
		3.37 per cent	2.88328E + 12	6.89	0.32		
				6.94	0.30		
72BI	0.641	14.80 per cent	5.00316E + 12	7.46	0.13	$\beta\text{D}$	$\beta 21/\text{R}$
		21.47 per cent	5.27253E + 12	7.86	0.12		
				7.69	0.13		

2b; Audin 1999). Thus, it was proposed that the Danakil and Ali Sabieh blocks became isolated  $>7$  Ma and proceeded to rotate in opposite senses, opening the depression in a saloon doors fashion (Courtilot 1980; Sichler 1980). No data were available to test this hypothesis for the Ali Sabieh part: this is one of the purposes of the present study.

In the same period, the Red Sea rift propagated towards the south, creating part of the Manda Hararo rift (MH; Lahitte *et al.* 2002). This intersected the pre-existing northern termination of the East African rift and the part of Africa to the south of the large escarpment was left relatively unaffected. Such was the situation 4 Ma (Kidane *et al.* 2003), when the Stratoid series was emplaced in Central Afar through a broad set of NW–SE trending fissures. The Stratoid formation covered most of the previous (Dahla) volcanic products, which now crop out only at the edges of the Afar depression.

Prior to the present study, there were only very few palaeomagnetic and geochronological data available from the Ethiopian side of the Ali Sabieh region. The chronological study of Zumbo *et al.* (1995), from the Djiboutian side only, was focused on the Stratoid basaltic series (younger than 4 Myr). Our aim was to sample as many sites as possible and to focus on the older series, in order to constrain the ages and rotations recorded by the different volcanic formations that surround the Ali Sabieh block. The fieldwork on which the present paper focuses was undertaken in 1996 and 1997, and the analytical work is described in detail in Audin (1999). In the following, we first describe the different geophysical approaches and the methods used, then the palaeomagnetic and geochronological results and, finally, discuss them in the framework of the regional tectonic setting.

### 3 METHODS AND RESULTS

#### 3.1 Geochronology

Eleven basaltic flows and two rhyolitic edifices of the Ali Sabieh area were sampled (Fig. 3) and processed for K-Ar and Ar/Ar dating in the UPS-IPGP geochronology laboratory at Orsay. Decay constants and isotopic ratios of Steiger & Jäger (1977) were used. Examination of thin sections of each selected basaltic flow confirmed the freshness of the lava and the absence of alteration phases. The rhyolitic samples were slightly weathered, which motivated us to perform extensive geochronological investigations, with both K-Ar and Ar/Ar analyses performed on multiple phases.

##### 3.1.1 K/Ar technique

The standard sample preparation procedure for the Cassinot technique was followed (Cassinot & Gillot 1982). For basalts, the groundmass was selected because of its higher K content and also because it crystallizes at the surface following eruption and therefore is the phase most likely to have equilibrated with the atmosphere. For rhyolites, the slight alteration present in the glassy matrix was eliminated by a prolonged ultrasonic cleaning using a 5 per cent nitric acid solution and heavy liquid separation in a narrow density range. Plagioclase and K-feldspar were also analysed.

K was measured by flame emission spectroscopy and Ar was measured with a mass spectrometer identical to the one described by Gillot & Cornette (1986). The  $^{40}\text{Ar}$  signal calibration is obtained from repeated analyses of the interlaboratory standard GL-O with the recommended value of  $6.679 \times 10^{14}$  atoms/g of  $^{40}\text{Ar}^*$  (Odin

**Table 2b.** K-Ar results for rhyolitic samples. Column headings indicate: Sample-phase (identification-mineralogical phase), K per cent (potassium concentration), per cent  $^{40}\text{Ar}^*$  (concentration of radiogenic  $^{40}\text{Ar}$ ),  $^{40}\text{Ar}^*$ (at./g; number of atoms of radiogenic  $^{40}\text{Ar}$  per gram), age (in Myr), Un. (uncertainty, in Myr). Ages in italic indicate rejected analyses (see text). For each site, weighted mean age and uncertainty are also indicated, site (palaeomagnetic site name), polarities (N: Normal, R: Reverse).

Sample-phase	K per cent	per cent $^{40}\text{Ar}^*$	$^{40}\text{Ar}^*$ (at./g)	Age (Myr)	Un. (Myr)	Site/Polarity
72AS-gdm	2.815	21.21 per cent	5.0241E + 13	17.0	0.3	
		23.63 per cent	5.0156E + 13	17.0	0.3	
		29.40 per cent	5.0635E + 13	17.1	0.2	
72AS-Kfsp	4.42	67.05 per cent	9.3077E + 13	20.0	0.3	
		90.32 per cent	9.2921E + 13	20.0	0.3	
		Mean 72AS:		20.0	0.3	$\rho\text{M5/N}$
72AH-gdm	4.212	35.21 per cent	8.9972E + 13	20.3	0.3	
72AH-Kfsp	5.021	31.61 per cent	1.0859E + 14	20.6	0.3	
		27.04 per cent	1.0550E + 14	20.0	0.3	
		Mean 72AH:		20.3	0.3	$\rho\text{M1/R}$

1982). Typical uncertainties of 1 per cent are reached for the  $^{40}\text{Ar}$  calibration and K content measurement. As already recognized for Stratoid basalts (Lahitte *et al.* 2001), the critical source of uncertainty comes essentially from the determination of radiogenic content. The detection limit of our system is 0.1 per cent of  $^{40}\text{Ar}^*$ , which makes the Cassinot technique (Cassinot & Gillot 1982) especially suitable for young and/or highly contaminated lavas.

K-Ar results are reported in Tables 2(a) and (b). Most analyses have been duplicated, except for units 72AL1, 72AL2 and 72AL, which are in stratigraphic order. In all cases, duplicates are compatible at the  $2\sigma$  level. Mean ages and uncertainties given in Table 2 have been weighted by the radiogenic content. They range from  $0.631 \pm 0.019$  to  $20.6 \pm 0.2$  Myr.

The multiphase analyses of the Mabla rhyolites showed incompatible ages for K-feldspar and groundmass of the 72AS unit, with values of  $20.0 \pm 0.3$  and  $17.0 \pm 0.2$  Myr, respectively. The latter should be considered with caution because the former is in agreement with the age of the other dated units. Both the 72AH groundmass and K-feldspar provided identical K-Ar determinations of  $20.3 \pm 0.3$  Myr. Plagioclase crystals from 72AH unit showed a strong resistance to HF etching during dissolution, which made accurate K content determination impossible.

### 3.1.2 $^{40}\text{Ar}/^{39}\text{Ar}$ technique

In order to bring additional support to the K-Ar ages obtained on multiple phases from the rhyolite of Ali Sabieh, we also performed  $^{40}\text{Ar}/^{39}\text{Ar}$  analyses on the same mineralogical preparations. Samples 72AH-plag., 72AH-gmd and 72AS-Kfsp (72AH-Kfsp) were irradiated for 50 h (60 h) in the fast neutron reactor of the University of Oregon. The J factor was determined using the HD-B1 biotite standard with the proposed age of 24.2 Myr (Hess & Lippolt 1994). Interfering reactions from Ca and K were monitored using  $\text{CaF}_2$  and  $\text{K}_2\text{SO}_4$  pure salts. Because of the low Ca content of these samples, these corrections appeared to be of limited effect on the age determinations. On the other hand, because for both runs the canister was not flipped halfway through the irradiation, the J factor displays more than 10 per cent variation within the 6 cm length of the tubes. Thus, the uncertainty attached to the J determination is

of the order of 2 per cent. The  $^{40}\text{Ar}/^{39}\text{Ar}$  technique is being used here to check the absence of perturbation since emplacement. The complete description of the multicollector system used in this study is given in Coulié (2001).

Four out of five step heating analyses display a relatively flat apparent age spectrum over a wide gas fraction, allowing the calculation of a plateau age (Fig. 4).  $^{40}\text{Ar}/^{39}\text{Ar}$  step heating data are given in Table 3 and Fig. 4. They show the apparent age spectra and the associated inverse isochrons. In all cases, the  $^{36}\text{Ar}/^{40}\text{Ar}$  intercept is of atmospheric composition at the  $2\sigma$  level and the isochron age agrees with the plateau age. Only the latter, with the total uncertainty (Table 3), will be considered in the following discussion. The three phases from 72AH volcanic unit show concordant plateau ages. The groundmass, K-feldspar and plagioclase phases display plateau ages of  $19.6 \pm 0.4$ ,  $19.9 \pm 0.4$  and  $20.4 \pm 0.6$  Myr, respectively. K-feldspar from unit 72AS gave a well defined plateau age of  $19.7 \pm 0.4$  Myr (Fig. 4). Sample 72AS-gdm, the groundmass phase from this unit, displayed a perturbed pattern with increasing ages from 15 to 20 Myr and a total gas age in agreement with the K-Ar age (Table 3). It is much younger than the K-feldspar age from this unit, suggesting that weathering (observed in thin section) perturbed the K and Ar retentivity of this phase.

### 3.2 Palaeomagnetism

A total of 46 sites were drilled in the field for palaeomagnetism and oriented *in situ* with a magnetic compass. As often as possible sun-compass orientation was also measured. At each site, at least seven cores (total = 550 samples) were collected near the center of the flow and with a distance of approximately 1 m between cores. Our sampling strategy was focused on the Somali, Dahla and Younger basalt formations in order to compare the results from this area with those obtained on the same formations north of the Gulf of Tadjoura around the Danakil block (Fig. 3). We also conducted a preliminary study on the Mabla formation to test their demagnetization pattern. All sites were selected in the field on the basis of their petrologic characteristics and geologic formation (Black *et al.* 1975; Varet & Gasse 1978). In six of the sampled sites,

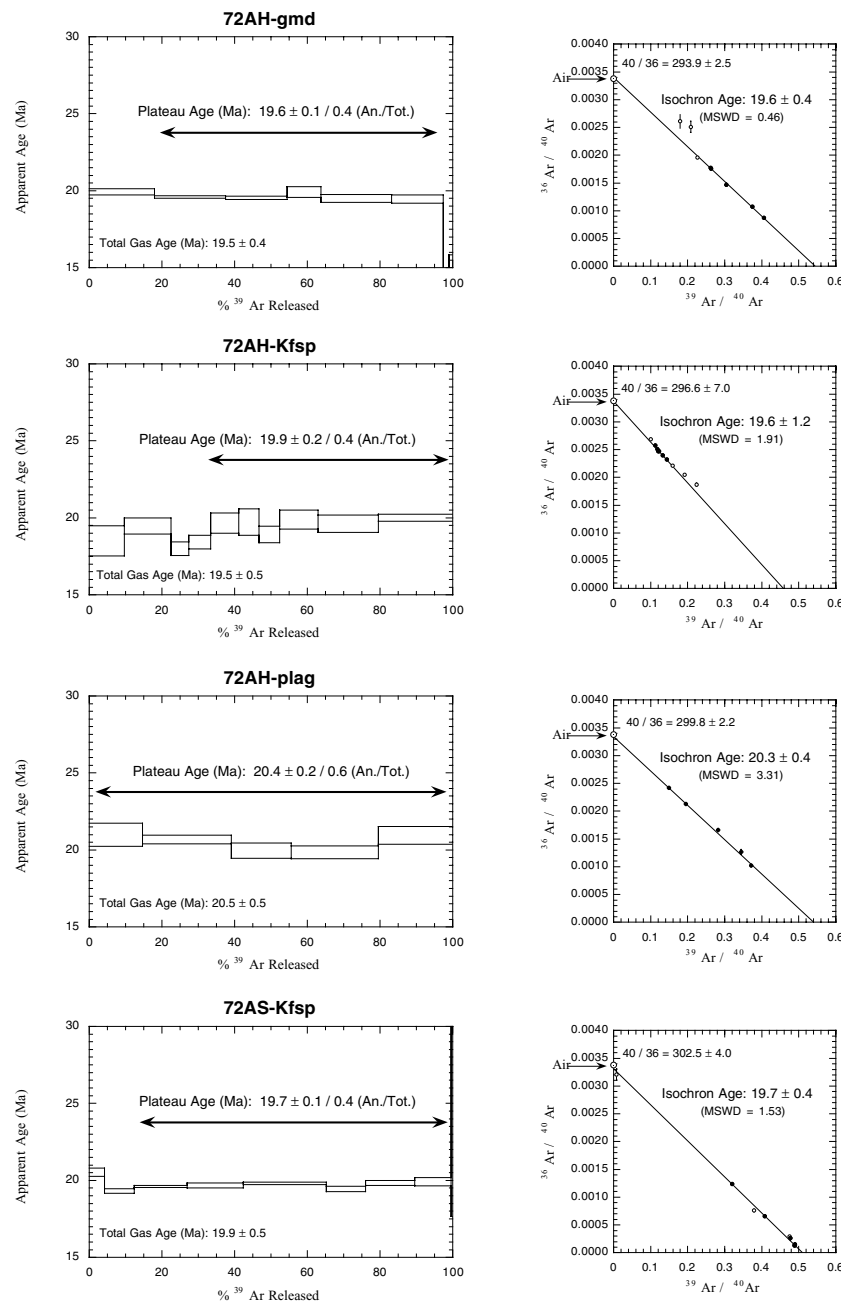


**Figure 4.**  $^{40}\text{Ar}/^{39}\text{Ar}$  apparent age spectra (in Myr) and associated inverse isochrons. The double arrows show the temperature steps included in the plateau age calculation. Analytical uncertainties (An.) using error propagation as described by McDougall & Harrison (1988); total uncertainty (Tot.) taking also into account the uncertainty in the J-factor determination (see text). The total gas age has been calculated by summing all the gas released. Isochron intercepts have been obtained using Mahon (1996). Mean square weighted deviation (MSWD).

structural characteristics (strike and dip) were carefully measured for tilt correction. When possible, sampling of superimposed flows was performed. In order to avoid flows struck by lightning, the uppermost flow from basaltic tables was not sampled. Back in the laboratory, 2.5-cm-diameter cores were cut into 2.2-cm-long samples, suitable for palaeomagnetic measurements. Measurements were performed in the shielded room of IPGP using a Geophysica-Brno JR5 spinner magnetometer. Samples were demagnetized either by alternating field in a Schönstedt instrument or thermally in Pyrox field-free furnaces.

The youngest Afar basalts, Stratoid and recent formations have been the subject of numerous, extensive research and can be consid-

ered here as a regional reference (Courtilot *et al.* 1984; Kidane *et al.* 2003). The initial Natural Remanent Magnetization (NRM) intensities were found to be typical of Afar basaltic formations, ranging from 0.26 to 98 A/m. As shown in Fig. 5, basaltic samples from the Dahla, Somali and Younger basalt formations are characterized by maximum unblocking temperatures below  $600^\circ\text{C}$ , most of them between 500 and  $580^\circ\text{C}$ . The median destructive field of NRM is apparently normally distributed, with a rather sharp mode in the 20–30 mT range (Audin 1999). In rare cases, such as A09-04A, the high value observed can be associated with a first component displaying an opposite polarity. These features suggest that a titanomagnetite is the main carrier of the remanence (Fig. 5).

**Table 3.**  $^{40}\text{Ar}/^{39}\text{Ar}$  isotopic data. Step #: incremental heating step number;  $^{40}\text{Ar}/^{39}\text{Ar}$ ,  $^{38}\text{Ar}/^{39}\text{Ar}$ ,  $^{37}\text{Ar}/^{39}\text{Ar}$ ,  $^{36}\text{Ar}/^{39}\text{Ar}$ : isotopic ratios;  $^{39}\text{Ar}$ :  $^{39}\text{Ar}$  signal (in  $10^{-12}$  mol.);  $^{40}\text{Ar}^*$ : radiogenic  $^{40}\text{Ar}$  content (in per cent); Un.  $^{40}\text{Ar}^*/^{39}\text{Ar}$ : analytical uncertainty; An. Un.: analytical age uncertainty (in Myr); Tot. Un.: 1 total age uncertainty (in Myr).

Step#	$^{40}\text{Ar}/^{39}\text{Ar}$	$^{38}\text{Ar}/^{39}\text{Ar}$	$^{37}\text{Ar}/^{39}\text{Ar}$	$^{36}\text{Ar}/^{39}\text{Ar}$	$^{39}\text{Ar}$ ( $10^{-12}$ .mol)	$^{40}\text{Ar}^*$ (per cent)	$^{40}\text{Ar}^*/^{39}\text{Ar}$	Un. $^{40}\text{Ar}^*/^{39}\text{Ar}$	Age (Myr)	An. Un. (Myr)	T. Un. (Myr)
72AH-groundmass: J = 5.96E-3											
1	4.4217	0.0127	0.0172	0.0087	3.3700	42.17	1.8647	0.0188	19.94	0.20	0.28
2	2.4617	0.0126	-0.0354	0.0021	3.6461	74.38	1.8309	0.0076	19.58	0.08	0.21
3	2.6729	0.0117	0.0009	0.0029	3.1655	68.35	1.8271	0.0094	19.54	0.10	0.22
4	3.2852	0.0132	-0.0091	0.0048	1.7564	56.65	1.8612	0.0328	19.90	0.35	0.40
5	3.8039	0.0129	0.0405	0.0067	3.6369	47.93	1.8232	0.0248	19.50	0.26	0.33
6	3.8135	0.0143	0.0092	0.0068	2.6436	47.71	1.8194	0.0256	19.46	0.27	0.33
7	4.8081	-0.0085	0.2234	0.0121	0.2975	25.89	1.2452	0.1497	13.34	1.60	1.60
8	5.5593	0.0139	1.7078	0.0151	0.1983	22.93	1.2767	0.2032	13.68	2.17	2.17
72AH-K feldspar: J = 5.01E-3											
1	9.9914	0.0129	-18.3474	0.0268	1.3809	20.64	2.0626	0.1100	18.56	0.98	0.98
2	6.2808	0.0136	-1.4286	0.0139	1.8286	34.55	2.1701	0.0579	19.52	0.52	0.52
3	4.4738	0.0159	-107.8901	0.0084	0.6959	44.82	2.0054	0.0488	18.05	0.44	0.44
4	5.2198	0.0121	2.0777	0.0107	0.8612	39.35	2.0539	0.0500	18.48	0.45	0.45
5	6.9634	0.0167	41.3938	0.0162	1.1100	31.46	2.1908	0.0741	19.71	0.66	0.66
6	8.4806	0.0173	112.7061	0.0213	0.7824	25.93	2.1993	0.0963	19.78	0.86	0.86
7	8.8926	0.0206	-22.0800	0.0230	0.8144	23.71	2.1083	0.0591	18.97	0.53	0.53
8	8.1872	0.0163	10.9303	0.0202	1.5016	27.08	2.2167	0.0681	19.94	0.61	0.61
9	7.5386	0.0144	-21.2862	0.0181	2.3782	28.99	2.1857	0.0629	19.66	0.56	0.56
10	8.2841	0.0136	-34.9797	0.0205	2.9107	26.93	2.2308	0.0257	20.07	0.23	0.23
72AH-plagioclase: J = 6.12E-3											
1	6.7206	0.0106	0.0104	0.0163	0.9277	28.45	1.9122	0.0683	20.99	0.75	0.77
2	2.6930	0.0113	0.0019	0.0027	1.5409	69.97	1.8843	0.0263	20.68	0.29	0.35
3	2.9071	0.0066	0.0046	0.0037	1.0378	62.51	1.8171	0.0460	19.95	0.50	0.54
4	3.5501	0.0126	0.0058	0.0059	1.5093	50.91	1.8074	0.0389	19.85	0.42	0.47
5	5.1415	0.0143	0.0012	0.0109	1.2899	37.11	1.9080	0.0542	20.94	0.59	0.63
6	142.8108	-0.1292	0.2402	0.4664	0.0244	3.52	5.0278	12.947	54.67	138.7	138.7
72AS-K feldspar: J = 5.60E-3											
1	2.6390	0.0117	0.0381	0.0020	0.7200	77.42	2.0433	0.0274	20.53	0.27	0.34
2	2.1037	0.0134	0.0225	0.0006	1.3721	91.37	1.9221	0.0155	19.32	0.15	0.25
3	2.0424	0.0107	0.0077	0.0003	2.4615	95.54	1.9513	0.0073	19.61	0.07	0.21
4	2.0448	0.0096	0.0125	0.0003	2.5982	95.76	1.9581	0.0171	19.68	0.17	0.26
5	2.0499	0.0113	0.0083	0.0003	3.8598	96.13	1.9706	0.0076	19.80	0.08	0.21
6	2.0945	0.0139	0.0081	0.0005	1.8223	92.36	1.9344	0.0168	19.44	0.17	0.26
7	2.4486	0.0105	0.0100	0.0016	2.2896	80.58	1.9731	0.0162	19.82	0.16	0.26
8	3.1293	0.0119	0.0198	0.0039	1.6764	63.35	1.9823	0.0268	19.92	0.27	0.33
9	124.1906	0.0680	-0.1197	0.3990	0.0839	5.04	6.2636	4.5644	62.20	44.5	44.6

Samples from the Mabla formation show rather low NRM intensities ranging from 0.03 to 1 A/m for rhyolites and from 0.3 to 5 A/m for basalts. Some basaltic samples, such as  $\rho\text{M4-06A}$ , have a component with low unblocking temperatures (150 °C), which can be interpreted as the result of a secondary overprint superimposed to the Characteristic Remanent Magnetization (ChRM) carried by a higher temperature component. The twin sample treated with the AF technique ( $\rho\text{M4-06B}$ ) also displays two opposite components that can, however, easily be interpreted using the Zijderfeld projections (Zijderfeld 1967 Fig. 5;).

In most cases, components were extracted using principal component analysis (Kirschvink 1980 Fig. 5;). When overlapping spectra are present, the Halls (1976) demagnetization circles method was preferred. The two data types were integrated following McFadden & McElhinny (1988). Low blocking field or temperature components generally average near the present field direction in Afar and

are likely the result of recent overprints. There was generally little ambiguity in extracting the more resistant characteristic remanent magnetization. As previously observed for Afar basalts (e.g. Kidane *et al.* 2003), the AF technique was more efficient at isolating the ChRM. Following pilot studies, 90 per cent of our samples were treated by this technique. Two sites, which exhibit high NRM intensity and/or large and chaotic scatter of NRM directions, were probably affected by lightning and were discarded.

## 4 DISCUSSION

### 4.1 Comparison with previous whole rock K-Ar and $^{40}\text{Ar}/^{39}\text{Ar}$ ages

As discussed by Lahitte (2000), many problems in interpreting ages from Afar were derived from the systematic whole rock K-Ar

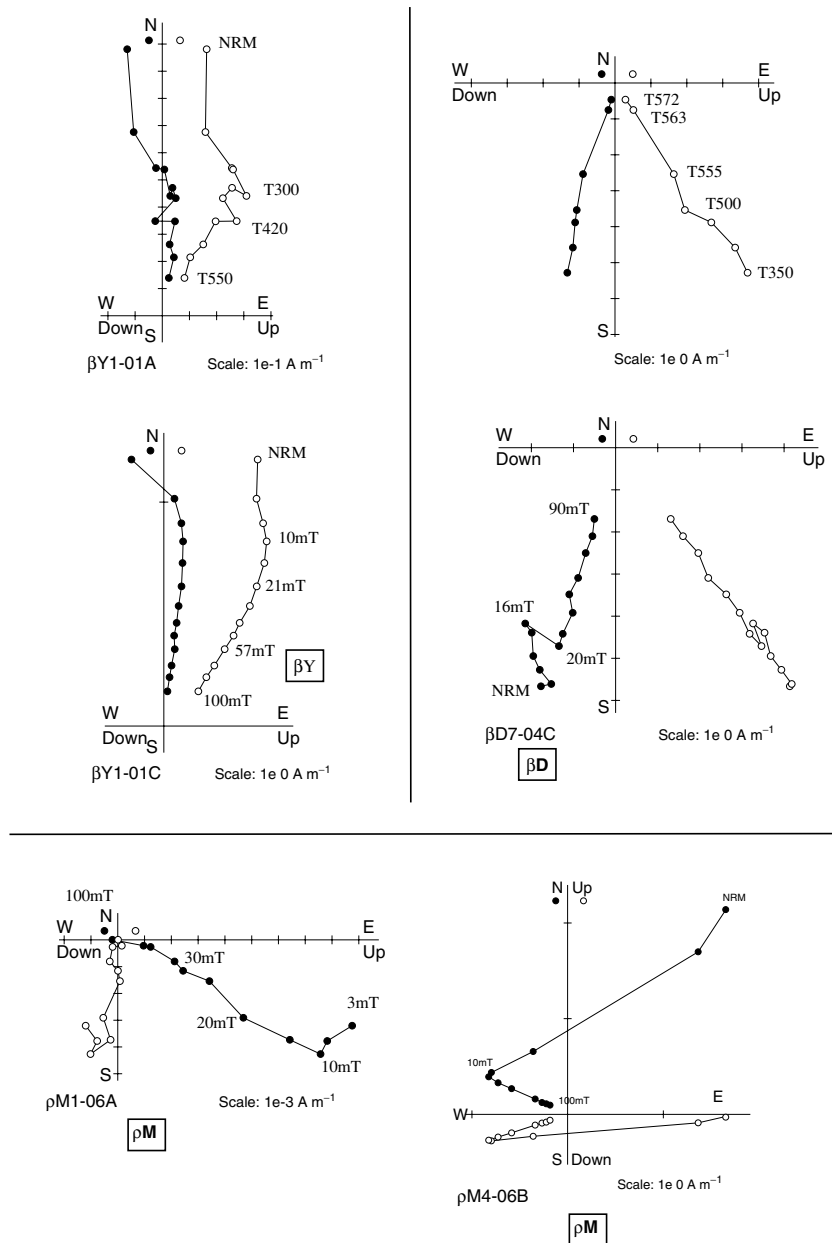


**Figure 5.** Palaeomagnetic vector plots for selected examples of each sampled volcanic formation: Zijdeveld (1967) diagrams for representative samples submitted either to thermal (T) or AF (mT) demagnetization.

dating performed in the 1970s. In addition to excess argon possibly incorporated in mafic phases, analyses of partly altered samples could have led to erroneous ages. This is especially true for the oldest formation, but has also been evidenced for recent flows from the Stratoid formation (Lahitte 2000). With these considerations in mind, together with the new age determinations of Table 2, the earlier results (Table 1; Varet & Gasse 1978) have been included in the following discussion. As presented below, the 13 new ages can be grouped with subsets, corresponding more or less to the previously identified geological formations.

#### 4.1.1 Younger basalts ( $\beta_y$ )

This group includes the recent basaltic formations (Gulf basalts and Stratoid basalts) and, at a larger scale, all basaltic lava flows younger

than 4 Myr sampled in this study (Pleistocene and Late Pliocene; Fig. 3). Our data are concordant with previous conventional K-Ar data obtained from ages from 0.5 to 4 Myr by Courtillot *et al.* (1984), but older ages attributed to the lower Stratoid series (Varet & Gasse 1978) were not found around the Ali Sabieh block. Moreover, they were not encountered by Lahitte *et al.* (2001) over a larger scale in central Afar, or by Zumbo *et al.* (1995) in Djibouti. Two basaltic flows dated here were sampled in the northern part of the Ali Sabieh block: 72AA and 72AO. They lie in what was previously mapped as the Dahla formation, next to the geological boundary between the Dahla basalts and the Stratoid and Gulf basalts, respectively (Fig. 3). Both ages are younger than 2 Myr (Table 2), clearly indicating that these sites belong to the Gulf basalts defined by Gasse *et al.* (1987). In the southern Ali Sabieh region, two additional sites located close to the Somalian escarpment (72BO, 72BF) were formerly mapped

**Table 4a.** Mean palaeomagnetic directions for sites <4 Myr old (here call Younger basalts) in the Ali Sabieh region (Djiboutian and Ethiopian part). Site (identification; prefix B and C, and 88, 89 after Courtillot *et al.* (1984);  $N$  = number of samples;  $D, I$  = declination and inclination in degrees (subscript  $g$  and  $s$  for stratigraphic and tilt corrected coordinates, respectively); n.d. (not determined);  $k$  and  $\alpha_{95}$  are statistical parameters from Fisher (1953); Pol. (magnetic polarity); Lat., Long. (geographic coordinates); n.a. (not available). The 12 lowermost sites were not taken in account in the mean direction determinations.

Site	$N$	$Dg$	$Ig$	$Ds$	$Is$	$k$	alpha95	Pol.	Lat.	Long.
$\beta Y3$	8	2.8	-7.7	2.8	-7.7	289.2	3.3	N	11.31	42.94
$\beta Y4$	6	.4	-9.6	.4	-9.6	83.1	7.7	N	11.31	42.94
$\beta Y6$	8	4.2	19.1	4.2	19.1	165.1	4.3	N	11.46	43.07
$\beta Y7$	6	177.8	-23.4	177.8	-23.4	286	4	R	10.80	42.59
$\beta Y8$	9	195.9	-6.7	197.4	-7.4	45.9	8	R	10.80	42.59
$\beta Y9$	7	186.4	-26.1	186.4	-26.1	288.6	3.6	R	10.75	42.62
$\beta Y10$	6	164.9	-9.8	164.9	-9.8	38.3	11	R	10.52	42.29
$\beta Y12$	6	202.9	-35	218.3	-30.4	160.1	5.3	R	9.75	41.87
$\beta Y13$	9	179.8	-20.5	179.8	-20.5	44.3	8.1	R	9.83	42.87
$\beta Y14$	9	187	-41.6	187	-41.6	89.7	5.5	R	9.92	42.15
$\beta Y16$	9	357.1	29.7	357.1	29.7	61.4	6.7	N	9.79	42.15
88	5	198	-23	195.5	-19	120	5.5	R	n.a.	n.a.
89	4	208	-24	208	-24	35	12	R	n.a.	n.a.
B6	6	198	-30	199	-24.5	82	8	R	n.a.	n.a.
B9	6	200	-27.5	197	-23.5	27	13	R	n.a.	n.a.
B10	9	195	-32	195	-32	34	9	R	n.a.	n.a.
B16	5	183	-20	183	-20	81	9	R	11.43	42.80
B14	4	189.5	-40	189.5	-40	26	13	R	11.14	42.17
C4	7	200	-30.5	200	-30.5	60	7.5	R	n.a.	n.a.
C7	8	173.5	-25	175	-25	35	9.5	R	11.28	42.65
C8	7	192	-27	192	-27	536	2.5	R	11.25	42.60
C9	8	191	-31	191	-31	76	6.5	R	11.26	42.47
C10	6	186.5	-3	187	9.5	147	5.5	R	11.13	41.95
C12	4	182.5	-12	177	-23.5	239	6	R	11.14	42.17
C23	6	178	3.5	178.5	0.5	434	3	R	11.00	42.33
C25	7	346	-1.5	346	3.5	121	5.5	N	11.15	42.40
$\beta Y1$	9	4.7	-40.7	4.7	-40.7	61.6	6.6	n.d.	11.51	42.87
$\beta Y5$	5	252.2	0.6	252.2	0.6	109.1	7.4	n.d.	11.40	43.00
$\beta Y11$	8	196.7	46.7	196.7	46.7	110.1	5.3	n.d.	10.46	42.26
$\beta Y15$	7	356.2	17	356.2	17	9.6	21.6	n.d.	9.83	42.15
$\beta Y2$	7	252.6	-3.6	252.6	-3.6	620.2	6.2	n.d.	11.31	42.94
B7	4	10	-55	10.0	-55	180	7	n.d.	11.51	42.80
B17	3	62	11	62	11	-	9	n.d.	11.43	42.80
B18	8	236	-0.5	236	-0.5	360	3	n.d.	11.43	42.80
C5	7	.5	-44	.5	-44	261	3.5	n.d.	11.51	42.80
C6	6	212.5	-34	213	-40	4	34	n.d.	11.50	42.72
C11	6	194	8	198.5	33.5	281	4	n.d.	11.13	42.17

as part of the Stratoid basalts, yet revealed unexpectedly young ages less than 1.5 Myr old (Table 2). These sites belong to an alignment of small volcanic cones along a normal fault set, topographically higher than the surrounding Stratoid lavas and showing a recent volcanic morphology (Figs 2 and 3). According to these ages, both flows can be associated with the recent reactivation of old WNW–ESE fissures located at the base of the Somalian escarpment and probably inherited from the early stages of the Afar opening process (Fig. 3).

#### 4.1.2 Dahla and Somali basalts ( $\beta D$ , $\beta So$ )

Four samples (72AZ2, 72AF, 72BE and 72BI) from the western boundary of the Ali Sabieh block (Fig. 3) yield ages in agreement with earlier 4 to 8 Myr K–Ar dating obtained for these formations (Table 1; Richard 1979; Gasse *et al.* 1987; Barberi *et al.* 1975; Chessex *et al.* 1975). Three other samples do not show the same agreement with previous age determinations. Flows 72AL, 72AL1

and 72AL2, sampled within a continuous section, are located on the eastern side of the Ali Sabieh block in the Somali basalt formation. They display ages ranging from  $2.67 \pm 0.06$  to  $2.93 \pm 0.08$  Myr, much younger than the Dahla formation. The  $\beta So$  (Fig. 3) are cropping out only on the Somalia side of the Ali Sabieh block and nowhere else in Afar. This formation was not recognized by Varet & Gasse (1978), but was described as a distinct series from isotopic dating and morphological constraints (Gasse *et al.* 1987). Following this dating approach, we can distinguish the Somali and Dahla formations. The former shows a well preserved surface morphology cut only by E–W flowing wadis ( $\beta So$ ; Fig. 3) and was not affected by tectonic features (Fig. 2). The latter, which is located on the north side of the Ali Sabieh block, is hardly deformed, suggesting that a major tectonic event, probably linked to the Danakil rotation, occurred locally on the Holhol fault system whereas the younger southern Somali basalts did not record this event (Audin 1999). For this reason, we choose to associate these three Somali flows with the Younger basalt group (see below for discussion).

**Table 4b.** Mean palaeomagnetic directions for Dahla sites in the Ali Sabieh region (Djiboutian and Ethiopian part). Site (B19 and C24 from Courtillot *et al.* 1984);  $N$  = number of samples;  $D, I$  = declination and inclination in degrees (subscript  $g$  and  $s$  for stratigraphic and tilt corrected coordinates, respectively);  $k$  and  $\alpha_{95}$  are the statistical parameters from Fisher (1953); Pol. (magnetic polarity); n.d. (not determined); Lat., Long. (geographic coordinates). 1 site was not taken into account in the mean direction determinations.

Site	$N$	$Dg$	$Ig$	$Ds$	$Is$	$k$	alpha95	Pol.	Lat.	Long.
$\beta D1$	7	174.5	-25.8	174.5	-25.8	179	4.5	R	11.43	42.8
$\beta D2$	10	184.7	-24.5	184.7	-24.5	33.3	8.5	R	11.43	42.8
$\beta D3$	7	34	10.6	34	10.6	101.7	6.2	N	11.28	42.69
$\beta D4$	6	183.2	-37	185.1	-34	154.1	5.5	R	11.14	42.47
$\beta D5$	5	.6	4.1	.8	1.2	255.8	4.8	N	11.14	42.47
$\beta D6$	10	11.3	12.4	11.7	9.1	22.3	10.5	N	11.14	42.47
$\beta D7$	8	17.5	-6.5	17.5	-6.5	226.6	3.7	N	11.17	42.57
$\beta D8$	10	18.5	6.7	18.5	6.7	245.2	3.3	N	11.17	42.57
$\beta D9$	8	20.7	3	20.7	3	127.5	5	N	11.21	42.67
$\beta D10$	6	338.6	-9.5	338.6	-9.5	34.4	12.4	N	11.18	42.93
$\beta D12$	6	175.7	-21.3	175.7	-21.3	39.9	10.7	R	11.22	42.95
$\beta D13$	6	9.7	17.8	9.7	17.8	120	6.3	N	11.34	42.95
$\beta D14$	6	33.1	-7.3	33.1	-2.4	61	8.6	N	11.26	42.76
$\beta D15$	6	34.3	18	34.3	18	197.8	4.8	N	11.35	42.72
$\beta D16$	7	12	24.5	10.8	29	160.1	4.8	N	10.85	42.64
$\beta D17$	8	182.1	-22.8	182.1	-22.8	846.6	1.9	R	10.84	42.63
$\beta D18$	7	181	-20.4	181	-20.4	58.1	8.1	R	10.84	42.63
$\beta D19$	9	183.9	-29.2	183.9	-29.2	219.5	3.5	R	10.84	42.62
$\beta D20$	7	182	-26.7	182	-26.7	240.8	3.9	R	10.84	42.62
$\beta D21$	11	197.7	-15.3	197.7	-15.3	75.5	5.3	R	10.24	42.51
B19	5	183	-18	183	-18	18	15	R	11.28	42.69
C24	4	195.5	-5	194.5	-13.5	161	7	R	11.1	42.33
$\beta D11$	6	212.5	-62.7	212.5	-62.7	4	9.5	n.d.	11.22	42.95

**Table 4c.** Mean palaeomagnetic directions for Mabla sites in the Ali Sabieh region (Djiboutian and Ethiopian part).  $N$  = number of samples;  $D, I$  = declination and inclination in degrees (subscript  $g$  and  $s$  for stratigraphic and tilt corrected coordinates, respectively);  $k$  and  $\alpha_{95}$  are statistical parameters from Fisher (1953); Lat., Long. (geographic coordinates).

Site	$N$	$Dg$	$Ig$	$Ds$	$Is$	$k$	alpha95	Lat	Lon
$\rho M1$	6	126.2	11.8	126.2	11.8	126.5	6.7	11.15	42.91
$\rho M2$	6	121.1	7.2	129.8	10.2	-	11	11.15	42.91
$\rho M3$	6	196	18.9	196	18.9	60.1	8.7	11.26	42.85
$\rho M4$	9	297.2	17.4	297.2	17.4	150	4.2	11.26	42.85
$\rho M5$	6	303	11.3	304.9	30.8	30	13.3	11.25	42.79

#### 4.1.3 Mabla formation ( $\rho M$ ) and $^{40}\text{Ar}/^{39}\text{Ar}$ ages

Mabla rhyolites 72AH and 72AS were dated with both argon based techniques on different mineralogical phases. Only the groundmass from 72AS did not provide a meaningful K-Ar age, nor a flat  $^{40}\text{Ar}/^{39}\text{Ar}$  age spectrum. The weighted mean (Taylor 1982) age of the three  $^{40}\text{Ar}/^{39}\text{Ar}$  analyses from 72AH is  $19.9 \pm 0.3$  Myr, in agreement at the  $1\sigma$  level with the K-Ar age of  $20.3 \pm 0.3$  Myr obtained from the groundmass and the K-feldspar separates. For 72AS-Kfsp, the K-Ar age of  $20.0 \pm 0.3$  Myr is also in agreement with the  $^{40}\text{Ar}/^{39}\text{Ar}$  age of  $19.7 \pm 0.4$  Myr obtained for this sample (Table 2b). It can be noted that our results are concordant with previous data in the range 17 to 19 Myr (Varet & Gasse 1978; Zumbo *et al.* 1995).

Ages corresponding to the younger part of the formation (*ca* 12 Myr) (Varet & Gasse 1978) were not found in this study. However, Chessex *et al.* (1975) have reported ages ranging between 9 and 14 Myr from samples taken around the Ali Sabieh block. To the south, near the Somalian escarpment, Coulié (2001) found rhyolitic domes with ages of approximately 12 Myr, in agreement with previous dating from the Mabla rhyolites also found south of the

Gulf of Tadjoura, within the southern Danakil block (Barberi *et al.* 1975).

The distribution of ages lead us to propose that two distinct periods of rhyolitic magmatic activity occurred around the Ali Sabieh block. A late one that can be associated with the Mabla series described in the southern Danakil block (approximately 10 to 13 Ma) and an earlier one which occurred between 17 and 25 Ma (Chessex *et al.* 1975). It should be noted that rhyolitic events are also identified in Afar between 26 and 20 Ma (Civetta *et al.* 1975; Varet & Gasse 1978). They are located just near the Miocene granitic plutons of Asa Ale in the northern part of the Danakil block, northeast of Sullu Adu, and around the Limmo Miocene granites, along the Ethiopian escarpment (Fig. 1). These coeval granitic plutons display clear intrusive contacts with the basement and were considered by Barberi *et al.* (1972) as the first volcanic events related to the initial stages of continental rifting which broke away the Danakil microplate. This rifting event is associated with rhyolitic effusion, which has dated as occurring around 20 Ma (Varet & Gasse 1978; Coulié 2001). In the Ali Sabieh region or even around the basement outcrop, no granitic bodies has been identified (Coulié 2001) but our dating of the rhyolitic domes, both east and west of the basement, revealed ages of

approximately 20 Myr. This could be interpreted as the signature of intrusive magmatic emplacements at depth. The 20 Myr old rhyolite lavas lie along the northern part of the basement outcrop in the Ali Sabieh region and spread along a NE–SW direction, parallel to the Holhol tectonic structure. It seems that pre-existing NE–SW trending tectonic structures have likely localized the effusion of these rhyolites in southern Afar. A more detailed discussion can be found in Coulié (2001).

#### 4.2 Comparison with the Geomagnetic Polarity Time Scale (GPTS)

The magnetic polarity of our dated sites is given in Table 4. First, it can be noted that the age determinations are all consistent at the  $2\sigma$  level (most of them at  $1\sigma$ ) with the distribution of the magnetic polarities (Fig. 6) according to the Geomagnetic Polarity Time Scale (GPTS) of Cande & Kent (1995). Five sites display normal

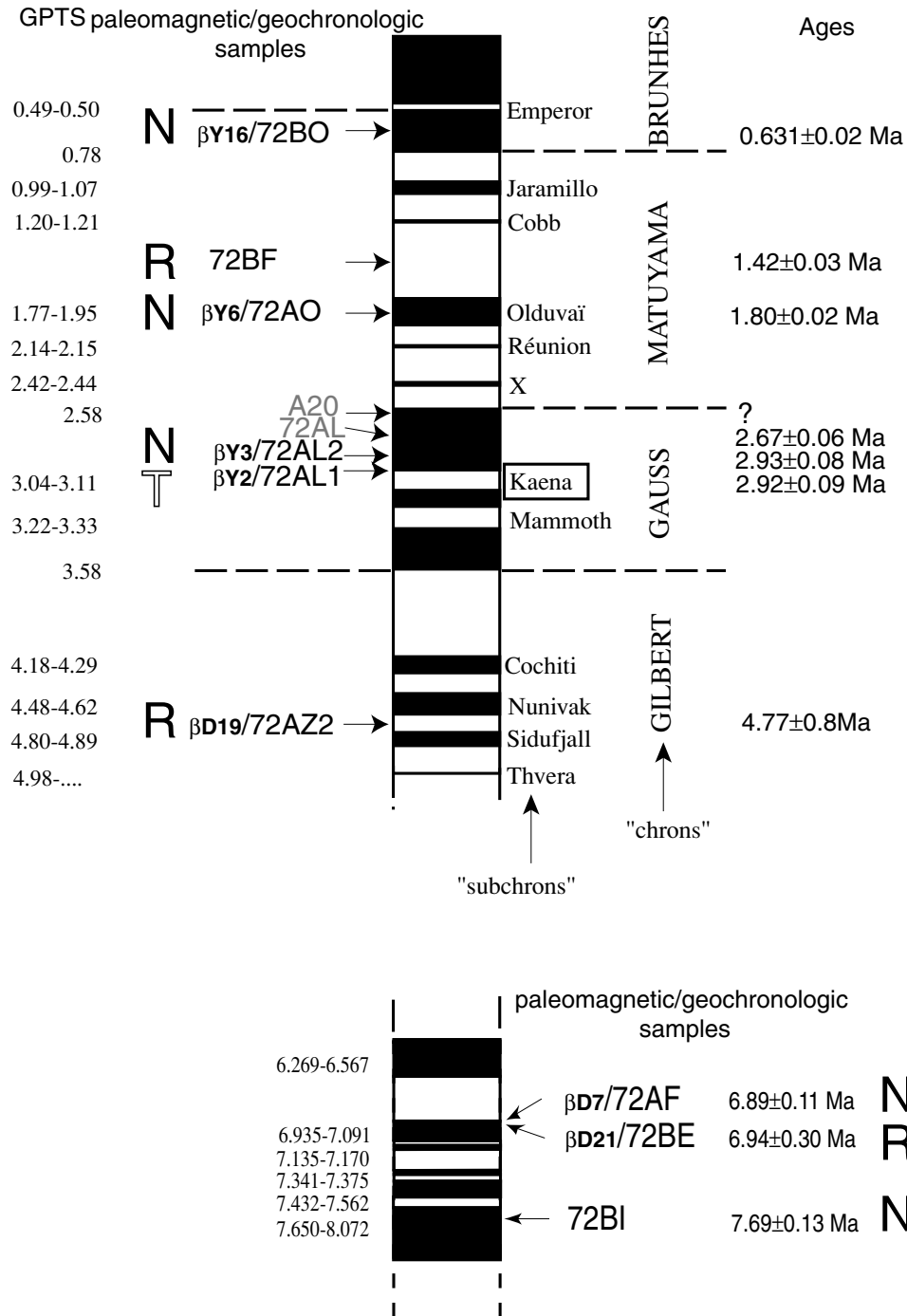


**Figure 6.** Comparison of our polarity/age results with the Geomagnetic polarity Geomagnetic Polarity Time Scale (GPTS; Cande & Kent 1995). Eleven ages obtained in this paper with  $1\sigma$  uncertainties. Chrons and subchrons are indicated, and also sample magnetic polarity (N = normal, T = transitional, R = reverse).

polarity, three display reverse polarity and one shows a transitional direction (Fig. 6). The latter,  $\beta Y2$ , is of particular interest because it comes from the only section with superimposed flows sampled here. Four flows from a Stratoid basalt section located south of the Holhol fault were investigated for palaeomagnetism and K-Ar dating. From bottom to top, site  $\beta Y2$  (dated at  $2.92 \pm 0.09$  Ma) directly underlines  $\beta Y3$  (dated at  $2.93 \pm 0.08$  Ma). A few flows above, 72AL, which was not sampled for palaeomagnetism, was dated at  $2.67 \pm 0.06$  Ma and is directly overlain by normal polarity site  $\beta Y4$ . This sequence unambiguously belongs to the C2An. In normal polarity interval (Fig. 6) from the Gauss chron (Cande & Kent 1995). The lowermost site ( $\beta Y2$ ) displays a transitional direction [virtual geomagnetic pole (VGP) latitude:  $17^\circ$ S] associated with a low field intensity value. Absolute palaeointensity determinations are not available but the average NRM displayed by samples from this site range between 1 and 2 A/m, four times lower than the upper flows from this sequence. Thus, abnormal directions and low remanent intensity strongly suggest that a transition has been recorded by this flow. Given the age of  $2.92 \pm 0.09$  Myr obtained (Tables 2 and 4), it is most probably the upper Kaena transition (Cande & Kent 1995). This is consistent with the K-Ar age of  $3.02 \pm 0.06$  Myr obtained by McDougall *et al.* (1992) in a fluvial sequence from East Africa and with the one of  $3.02 \pm 0.01$  Myr derived from astronomical calibration of sapropels in the Mediterranean (Hilgen 1991).

### 4.3 Mean palaeomagnetic site directions

Flow mean directions were calculated from at least four stepwise demagnetized samples. Palaeomagnetic directions and Fisher (1953) statistical parameters are listed in Table 4. Palaeomagnetic sites have been grouped by geological formation, determined either by their sampling position in previously identified formations (Varet & Gasse 1978) or from the new age determinations (Table 2). As described above, three formations have been identified in the Ali Sabieh area. Samples from the Somali basalts were here either attributed to the Younger basalts or the Dahla basalts subdata set as a function of their age and stratigraphic position (Fig. 3).

#### 4.3.1 Younger basalts ( $\beta_y$ )

Eighteen new palaeomagnetic directions have been obtained for this formation (labelled  $\beta Y$  in Table 4a). In addition, 21 sites from previous studies (Courtilot *et al.* 1984) sampled in the northern part of the Ali Sabieh block, have been incorporated in Table 4(a). Two sites ( $\beta Y1$  and C6), which show poorly defined mean directions with  $\alpha_{95}$  confidence cones larger than  $15^\circ$ , were not considered further. Because rotations are investigated here, we rely on the difference between the measured and expected ( $21^\circ$ ) inclination values in order to discard transitional field directions. A total of 5 sites ( $\beta Y1$ ,  $\beta Y11$ , B7, C5 and C11) with an inclination anomaly exceeding  $50^\circ$  have been removed. In addition, two sites ( $\beta Y5$  and B18) showing a very anomalous declination, between  $230^\circ$  and  $260^\circ$ , have not been considered. Site 72AA, which yielded a non-Fisherian distribution (Fisher 1953), with very high NRM values (44 A/m) suggesting that remagnetization as a result of lightning occurred, was also removed. Finally, site B17 was not included because of the low number of available cores ( $N = 3$ ). The directions of the 26 remaining sites are shown in Fig. 7(a). They yield a mean direction of  $D = 6.9^\circ$ ,  $I = 19.9^\circ$ ,  $\alpha_{95} = 6.5^\circ$  (Table 5) in stratigraphic coordinates, i.e. after tectonic correction (note however that, in the present case, flows are essentially flat lying). The mean directions calculated independently

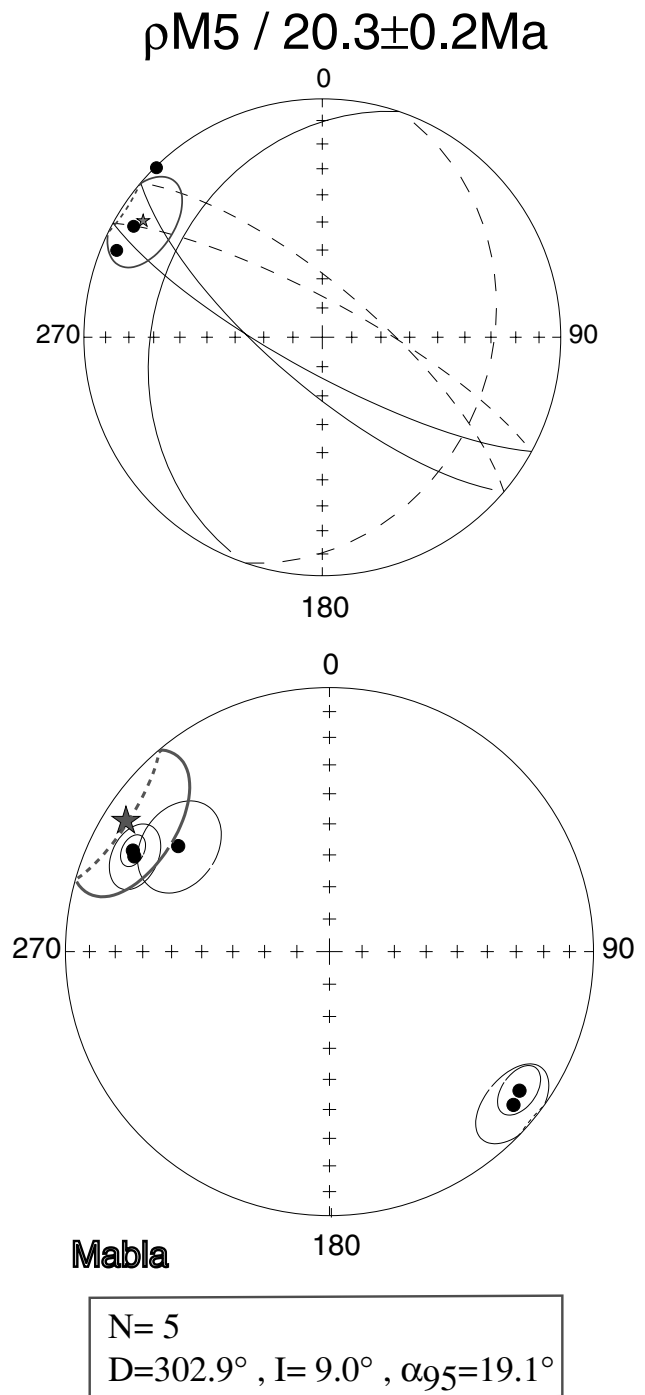


**Figure 7.** Stereographic projections of characteristic magnetization directions from sites of the Ali Sabieh area (a) Younger basalts: younger than 4 Myr; (b) Dahla basalts: 4–8 Myr. Mean directions of magnetization (shown with a star) with 95 per cent confidence interval. Values are given in inset. (c) Projection of means from region north (N) and south (S) of Holhol fault, shown for the two age groups (see text).

for the Gulf basalts, Stratoid basalts or Somali basalts are statistically indistinguishable.

#### 4.3.2 Dahla and Somali basalts ( $\beta_D$ , $\beta_{So}$ )

Before the present study was conducted, only two sites (B19 and C24, in Table 4b) from the northern Ali Sabieh area had been

**Table 5.** Mean palaeomagnetic directions and virtual geomagnetic pole (VGP) statistics. Data set [with their respective position to the Holhol fault; north-b: data from Courtillot *et al.* (1984) removed (see text)];  $D$  moy (mean declination);  $I$  moy (mean inclination);  $\alpha_{95}$  (Fisher (1953) statistical parameter); VGP lat. and VGP long. (geographic coordinates of the mean VGP); Disp. VGP (dispersion of VGPs around the mean pole).

Data set	$N$	$D$ moy	$I$ moy	$\alpha_{95}$	VGP lat.	VGP long.	Disp. VGP
Mabla formations ( $\rho M$ )							
All	5	302.9	9.0	19.1			
Dahla ( $\beta D$ ) and Somali ( $\beta So$ ) basalts							
All	22	10.0	15.4	7.0	79.9	149.5	15.0
North	13	15.1	12.2	9.1	74.5	149.6	14.5
South	9	2.3	19.7	10.2	87.6	148.2	12.7
Younger basalts ( $\beta_y$ )							
All	26	6.9	19.9	6.5	83.0	134.3	14.3
North	15	8.6	21.4	8.1	81.3	130.4	13.1
North-b	9	1.8	18.0	11.8	87.5	169.3	12.3
South	11	4.7	17.8	11.7	85.1	143.8	16.2
North-b & south	20	3.6	18.7	7.4	86.3	145.1	14.4

sampled in the Dahla formation (Courtillot *et al.* 1984). Twenty-three new sites (labelled  $\beta D$ ) obtained here are reported in Table 4(b). Using the same selection criteria as for the Younger basalt formation, others sites (for example,  $\beta D11$  and 72BI) were excluded from the following analyses. Site  $\beta D11$  was removed because it displays an inclination anomaly larger than  $40^\circ$  (Table 4b). Fig. 7(b) shows the remaining 22 sites and their mean direction ( $D = 10.0^\circ$ ,  $I = 15.4^\circ$ ,  $\alpha_{95} = 7^\circ$ ; Table 5) in stratigraphic coordinates, i.e. after tectonic corrections (expected direction after Besse & Courtillot 2002):  $D = 2.8^\circ$ ,  $I = 16.8^\circ$ ,  $\alpha_{95} = 3^\circ$ .

#### 4.3.3 Mabla formations ( $\rho M$ )

Five sites ( $\rho M1$ ,  $\rho M2$ ,  $\rho M3$ ,  $\rho M4$  and  $\rho M5$ ) were sampled from the Mabla series (Fig. 8). As shown in Table 4(c), relatively well defined directions have been obtained for these rhyolitic flows. They show rather straightforward demagnetization patterns, which in five cases allow to determine an average component (Figs 5, 8 and 9). For one site,  $\rho M2$ , we used the Halls (1976) demagnetization circles method only to identify the characteristic component of magnetization. Fig. 8 shows that the normal and reversed directions are more or less antipodal and, thus, can be used to calculate the mean direction  $D = 302.9^\circ$ ,  $I = 9.0^\circ$  ( $\alpha_{95} = 19.1^\circ$ ,  $N = 5$ ). Because it is far from the expected dipole direction, it is difficult to interpret this result in terms of tectonic deformation. Effectively, a clockwise rotation of more than  $100^\circ$ , or a counter-clockwise one of more than  $60^\circ$ , is necessary to account for this direction. It can be noted that in the latter hypothesis, the Mabla rhyolites found on the NE side of the Ali Sabieh block would be lined up with those found to the southeast of the Ali Sabieh block (Fig. 3). However, in the absence of additional data from more widespread sites ( $N = 4$  is actually too small to draw robust conclusions) to better constrain the mean direction obtained here, we prefer not to draw any tectonic interpretations for the Mabla formation.

#### 4.4 Horizontal rotations and regional domains

An average declination has first been calculated for all sites from the Dahla and Younger basalt formations in order to investigate horizontal rotations (Table 5; Figs 8 and 9). However, more insight can be

inferred when data are grouped with respect to their location relative to the Holhol fault, which delimits the domains we defined above (Figs 3 and 10). Approximately 10 sites are located on each side of this fault, for each time interval considered here, which allows significant mean palaeomagnetic directions to be calculated. For the Dahla basalts (8 to 4 Ma), 9 sites from the southern compartment display a declination of  $2.3 \pm 10.8^\circ$ , while 13 sites from the northern side yield a declination of  $15.1 \pm 9.3^\circ$ . Note that for the latter subset the reversal test (McFadden & Lowes 1981) is negative, probably as a result of the too small number of flows with reverse polarity ( $N = 5$ ) for averaging secular variation. Compared with the reference pole of Besse & Courtillot (2002) for this time interval, these results suggest a small clockwise rotation of approximately  $12 \pm 9^\circ$  for the northern Dahla basalts. Similarly, for the Younger basalt formation (4 to 0.5 Ma), no rotation can be deduced from the mean of  $4.7 \pm 12.3^\circ$  ( $N = 11$ ) calculated for the southern compartment and 15 sites located in the northern compartment of the Holhol fault (Figs 8 and 10) show a mean declination of  $8.6 \pm 8.7^\circ$ . Six sites (C4, B6, B9, B10, 88 and 89) out of 15 from the latter group can be considered as belonging to the blocks of Hanle and Gamarri inside the overlap zone (Courtillot *et al.* 1984) and therefore might have been affected by the recent tectonic activity leading to clockwise rotation linked to the bookshelf faulting mechanism (Tapponnier *et al.* 1990) (Figs 1, 8 and 10). When we remove these sites, a mean declination of  $1.8 \pm 12.4^\circ$  is obtained for the remaining nine sites (north-b in Table 5; Fig. 10). This brings additional support for the absence of tectonic deformation affecting the Younger basalt formation from the northern compartment of the Holhol fault for the last 4 Myr. Although uncertainties are rather large, partly as a result of the limited number of sites, we suggest that no significant rotation occurred in the southern compartment of the Holhol fault for the last 8 Myr; the northern compartment was rotated clockwise in the 8 to 4 Ma time interval, but no significant rotation occurred in the 4 to 0 Ma interval.

We also calculated the angular standard dispersion of VGPs using the same time frames and geographical grouping with respect to the Holhol fault (Table 5). This parameter was then compared to the expected value at Afar latitude (Angular Standard Dispersion =  $13.5 \pm 1^\circ$ ), based on palaeosecular variation models and the volcanic database for the last 5 Myr (Quidelleur & Courtillot 1996).

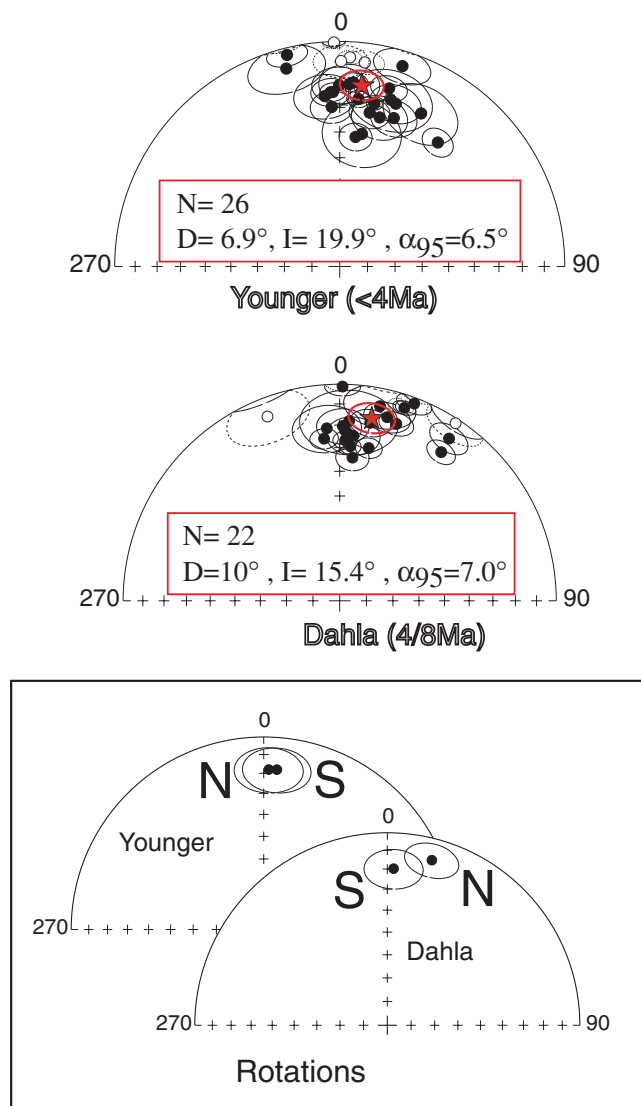


**Figure 8.** Stereographic projection of characteristic magnetization directions from rhyolitic sites of the Ali Sabieh area (rhyolitic and basaltic series belonging to the Mabla formation). Mean direction of magnetization (shown with a star) with the 95 per cent confidence interval. Values are given in inset.

The unrotated Dalha basalts from the southern compartment display a dispersion of  $12.7^\circ$ , lower than the one ( $16.2^\circ$ ) calculated for the Younger basalts from the same area. When grouped together, the VGP dispersion is  $14.4^\circ$  (20 sites), in good agreement with the expected value. For both groups from the northern compartment (rotated and unrotated sites, from Dalha and Younger basalts, respectively), the dispersions of VGPs ( $14.5^\circ$  and  $13.1^\circ$ , respectively; Table 5) are also in agreement with the expected value. Secular variation therefore seems to have been properly sampled in each of our subgroups, implying that internal deformation within each block and age range is not significant. Therefore, most of the deformation of the northern compartment of the Holhol fault that occurred during the 8–4 Ma interval must have been concentrated along existing strike-slip segments. This observation is consistent with the proposal that Afar tectonics are mostly accommodated at block margins (i.e. Tapponnier *et al.* 1990; Manighetti *et al.* 1998).

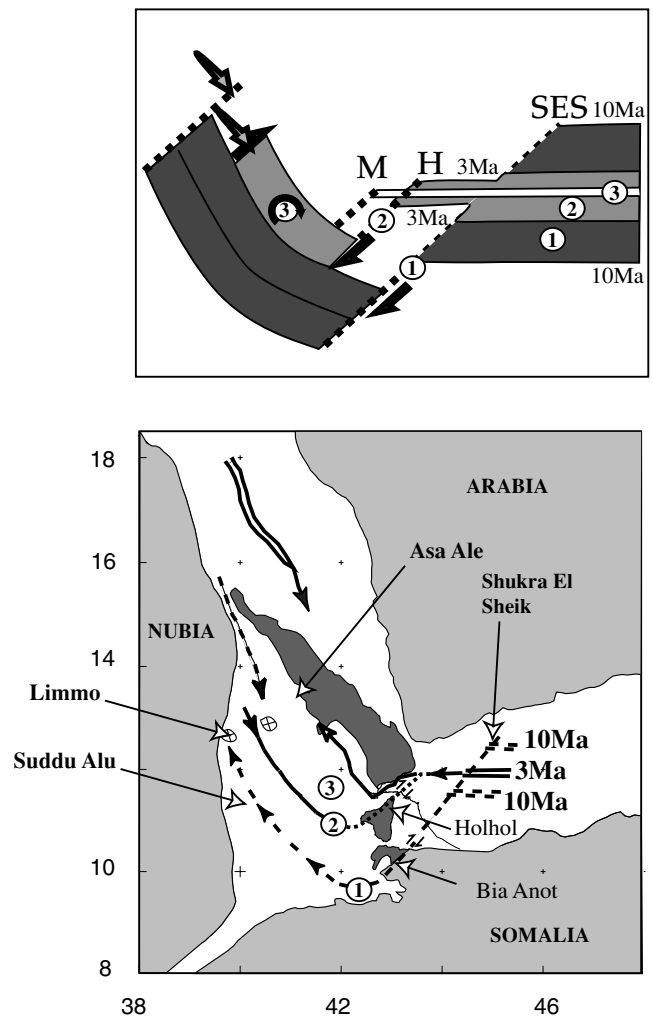


**Figure 9.** New model of rift propagation and transfer, including three steps of penetration from east to west of the Aden propagator within the Afar depression. Step 1: from 10 to 4 Ma; step 2: from 4 to 1 Ma; step 3: from 1 to 0 Ma (stage of deformation with bookshelf faulting). (1) and (2): Localized rift segments. (3) Bookshelf mechanism and diffuse deformation between localized rift segments. Site of Awash hominids from WoldeGabriel *et al.* (2001).

## 5 CONCLUSIONS: A CHRONOLOGY OF RIFT PROPAGATION AND TRANSFER IN AFAR SINCE CONTINENTAL BREAKUP

Since 30 Ma (e.g. Hofmann *et al.* 1997; Coulié *et al.* 2003), the Ethiopian plume head has influenced a vast area of NE Africa. A major ridge system extending from the Indian ocean propagated in a W–SW direction, along a path of least resistance (Manighetti *et al.* 1998). Following an initial phase of incipient breakup along the East African and Red Sea rifts (Courtillot *et al.* 1987), the Gulf of Aden rift began its propagation from the Indian ocean towards the hotspot area and arrived on the Shukra El Sheik (SES) discontinuity approximately 20 Ma [Figs 1, 2 and 9; Cochran (1981); Courtillot *et al.* (1987); Audin (1999)]. In the meantime, the Red Sea rift apparently propagated southwards, again also in the general direction of the hotspot area (Courtillot *et al.* 1987; Izzeldin 1987). As both propagators arrived near the junction area (*ca* 20 Ma), the Afar depression started to stretch and open through both localized (disconnected rift

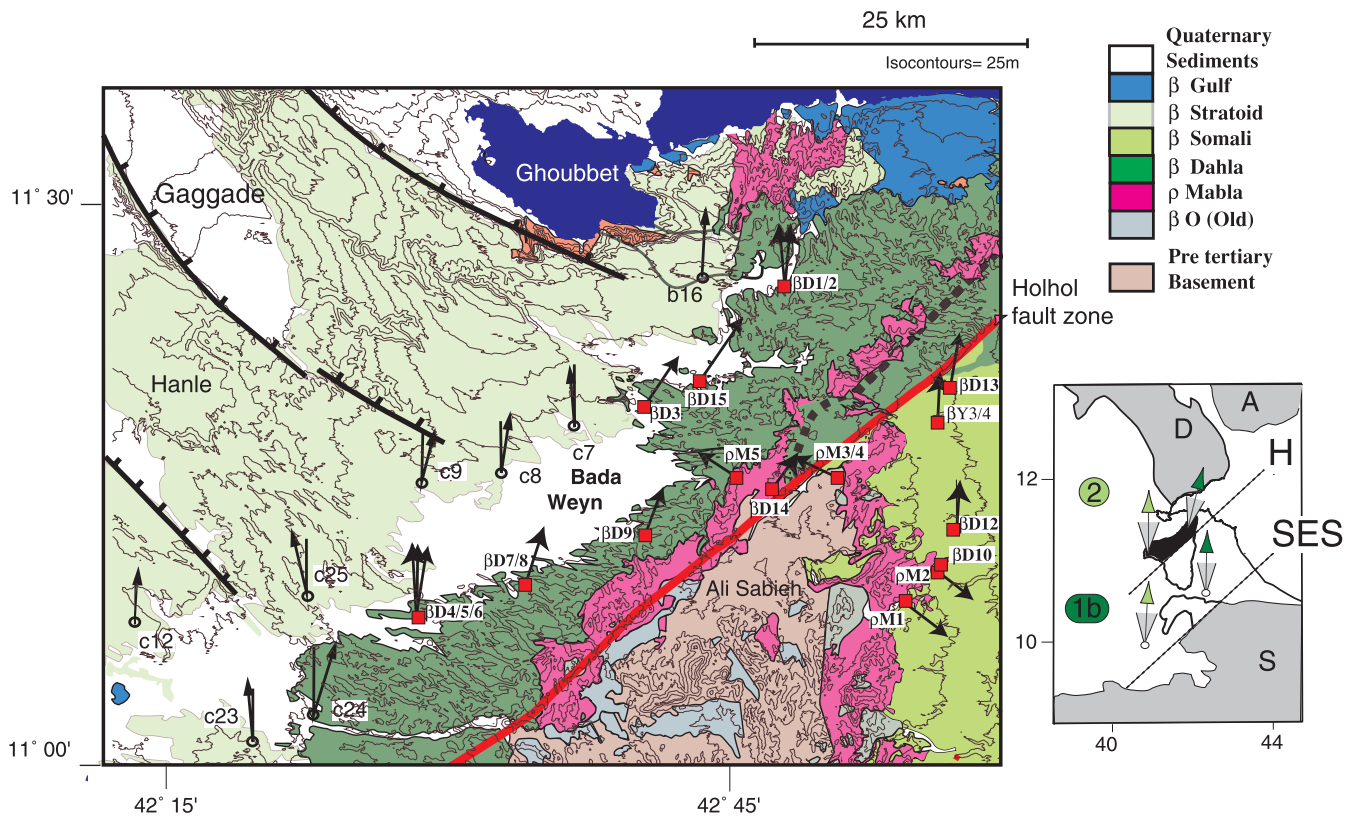


**Figure 10.** Detailed map with sites from the northern part of the Ali Sabieh block. Topographic contours superimposed on geological map. Same legend as Fig. 3. Mean direction obtained in each site is indicated by an arrow (squares after this study, circles after Courtilot *et al.* 1984). Inset: mean directions obtained for the blocks respectively north and south of the Holhol fault zone are indicated by a rotated colored arrow (dark green for step 1; green for step 2, steps after Fig. 10 and see text). Holhol fault zone (H); Shukra El Sheik fault zone (SES); Danakil block (DAN); Arabia (ARA); Somalian plate (SOM).

segments) and diffuse faulting, associated with magmatism (Audin 1999). Two microplates, the Danakil and Ali Sabieh blocks, were isolated (*ca* 10 Ma) and the depression started to open (Figs 2 and 9).

In the last 4 Myr, tectonic evolution has been dominated by rotation induced by bookshelf faulting in central Afar (Tapponnier *et al.* 1990). Since approximately 1 Ma, the Aden rift was localized inland, along the western edge of the Danakil block, where it has been propagating northwards (Fig. 1 and step 3 of Fig. 9). In the mean time, the already established Manda-Hararo rift (step 2 of Fig. 9), the southern termination of the Red Sea ridge system, propagated southwards along the western edge of the Afar depression, now the Ethiopian escarpment (*i.e.* Lahitte *et al.* 2002). In the process, a large overlap was formed (Figs 1 and 2; Manighetti *et al.* 2001). The strain history can be described in terms of rotations of small rigid blocks around vertical axes (Courtilot *et al.* 1984; Kidane *et al.* 2003). Two recent phases of deformation, evidenced by propagation and overlap, have been identified. At least five blocks rotated during the last 1 Myr, in such a way that they broke along their western ends, the eastern boundary of the overlap zone being anchored to the Ali Sabieh microplate (Figs 1 and 2; Manighetti *et al.* 2001).

It has been proposed that early propagation in what was to become the Gulf of Aden was the result of an episodic process, resulting mainly from complex interactions between 3-D plate geometry and the direction and intensity of the regional stress. It was first rapid (less than  $10 \text{ cm yr}^{-1}$ ), then slowed down (to a few  $\text{cm yr}^{-1}$ ) as the Aden rift reached the plume area 10 Ma and finally stalled along pre-existing discontinuities (Manighetti *et al.* 1998). This study has

allowed us to clarify the ill-known period from 10 to 4 Ma. Incorporating the data obtained in this paper in the general scheme of Audin (1999), an updated kinematic model of propagation and transfer of extension within southern Afar since 10 Ma can be proposed (Fig. 9).

After a series of systematic jumps to the south, rifting propagated into the proto-Gulf of Aden and stalled on the SES discontinuity from 20 to 10 Ma (Fig. 9a). Anomaly 5 (*ca* 10 Ma) is the oldest magnetic anomaly identified east of the SES discontinuity in the Gulf of Aden (Cochran 1981; Audin *et al.* 2001). Surprisingly, on the western side of the SES discontinuity, clear magnetic anomalies are identified only back to anomaly 2 (*ca* 3 Ma; Fig. 9; Audin 1999; Audin *et al.* 2001). This sudden loss of the oldest series of anomalies implies that a major rheologic and structural boundary must occur along the SES and its southern extension, the Bia Anot fault systems (Figs 2 and 9). As spreading was transferred into Afar by the SES—Bia Anot transform, extension became localized at the base of the present-day Ethiopian escarpment approximately 10 Ma and then propagated northwards inside the proto-Afar depression (from 10 to 4 Ma; step 1 of Fig. 9). During this stage, it seems likely that continental lithosphere was first stretched over a broad area and that localization of deformation with formation of an axial rift (in the Sullu Adu area) occurred only afterwards, between 8 to 4 Ma, during Dahla basalt emplacement (Fig. 9).

Unfortunately, in central Afar, the thick Stratoid series now covers most of these structures. Some evidence can be inferred from re-activated E–W faults, basins and neo-volcanic alignments (Fig. 2b) lying between the Somalian escarpment and the SE limit of the zone affected by bookshelf faulting (Audin 1999). Evidence for the

occurrence of volcanism and marginal graben formation from 7 to 5 Ma have been found along the Somalian escarpment (41°E; Chernet *et al.* 1998). Recent studies of hominid fossil-bearing formations in the Awash lowlands (Fig. 9b) yield ages between 6 and 6.5 Myr for underlying basalts (WoldeGabriel *et al.* 2001). In addition, Ukstins *et al.* (2002) reports a volcanic hiatus from 9 to 4 Ma in Yemen, which could correlate with the transfer of extension and localization of tectono-volcanism in southern Afar during step 1 of our model. The palaeomagnetic data acquired around the Ali Sabieh block provide new insights for the last 8 Myr interval. The domain south of the Holhol fault zone did not record any rotation, whereas the domain to the north experienced approximately 15° of clockwise rotation between 8 to 4 Ma. Such rotation may be linked to the 11° counter-clockwise rotation observed for the Danakil block since approximately 7 Ma (Manighetti *et al.* 2001). We propose that, as a result of the strain associated with the first stage of propagation into Afar (Fig. 9), the early Danakil block was split in two along the Holhol fault system approximately 8 Ma. The larger piece corresponds to the present-day Danakil block, the smaller fragment being bounded by the Maskali transform fault to the north and by the Holhol transform fault to the south (see also Audin 1999).

Thus, during step 2 (from 4 to 1 Ma; Fig. 9), as the Aden ridge crossed the SES discontinuity, the transfer along the SES—Bia Anot transform fault was abandoned. Another transfer started on the Holhol system, as the spreading center stalled at the southern tip of the Danakil block (Fig. 9). Because no rotation has been identified south of the Holhol fault since 8 Ma in the present study, it can be inferred that the Bia Anot and Holhol fault systems were not active simultaneously (Fig. 9). The absence of rotation during the interval 4–1 Ma in the northern domain suggests that only the strike slip Holhol fault was active during step 2. Finally, similar to what has been proposed by several authors for the SES discontinuity (step 1 of Fig. 9; Audin *et al.* 2001; Manighetti *et al.* 2001; Kidane *et al.* 2003), we suggest that propagation of the Aden ridge into Afar during the last 1 Myr stalled along the Maskali transform fault and then transferred through the Gulf of Tadjoura to the Ghoubbet rift zone (step 3 of Fig. 9).

In conclusion, recent acquisition of palaeomagnetic and geochronologic data in central eastern Afar, on the edges of the Ali Sabieh block, provides some of the last missing steps between the main phases of rift propagation in the Gulf of Aden (between 20 and 10 Ma) and the most recent activity since eruption of the Stratoid basalts (4 Ma to the present). The previously ill-known period between 10 and 4 Ma, for which most information has been drowned under the Stratoid lavas, appear to be one of discrete, successive steps in which the main Aden propagator stalls, transfers its motion to the southwest, triggers extension in south central Afar, then jumps westwards, stalls again and transfers again to the south. The lacerated structure of Afar volcanics, with its rotated stripes and blocks, was generated by this dual (rift plus transfer zone) propagating and jumping mode of deformation, which will eventually lead to complete continental breakup.

## ACKNOWLEDGMENTS

This work took place in the frame of a collaboration programme that was established between INSU-CNRS in France, the Department of Geology and Geophysics of the University of Addis-Ababa in Ethiopia and ISERST in Djibouti. The palaeomagnetic software PaleoMac used in this study was developed by J. P. Cogné (2003). This is LGMT 44.

## REFERENCES

- Audin, L., 1999. Pénétration de la dorsale d'Aden dans la dépression Afar entre 20 et 4 Ma, *PhD thesis*, Université de Paris 7 et Institut de Physique du Globe de Paris, Paris.
- Audin, L., Manighetti, I., Tapponnier, P., Métivier, F., Jacques, E. & Huchon, P., 2001. Fault propagation and climatic control of sedimentation on the Ghoubbet rift floor: Insights from the Tadjouraden cruise in the western Gulf of Aden, *Geophys. J. Int.*, **144**, 391–413.
- Baker, J.A., Snee, L.W. & Menzies, M.A., 1996. A brief Oligocene period of flood volcanism in Yemen; implications for the duration and rate of continental flood volcanism at the Afro-Arabian triple junction, *Earth planet. Sci. Lett.*, **138**(1–4), 39–55.
- Barberi, F., Tazieff, H. & Varet, J., 1972. Volcanism in the Afar depression: its tectonic and magmatic significance, *Tectonophysics*, pp. 19–29.
- Barberi, F., Ferrara, G., Santacroce, R. & Varet, J., 1975. Structural evolution the Afar triple junction, in *Afar Depression of Ethiopia*, **1**, pp. 38–54, eds Pilger, A. & Roesler, A., E. Schweizer. Verlagsbuchhandl. (Naegle u. Obermiller), Stuttgart, Germany.
- Besse, J. & Courtillot, V., 2002. Apparent and true polar wander and the geometry of the geomagnetic field over the last 200 Myr, *J. geophys. Res.*, **107**, Art. No. 2300.
- Beydoun, Z.R., 1970. Southern Arabia and Northern Somalia: comparative geology, *Phil. Trans. R. Soc. Lond.*, A. **267**, 267–292.
- Black, R., Morton, W.H. & Rex, D.C., 1975. Block tilting and volcanism within the Afar in the light of recent K/Ar age data, in *Afar Depression of Ethiopia*, **1**, pp. 296–300, eds Pilger, A. & Roesler, A., E. Schweizer. Verlagsbuchhandl. (Naegle u. Obermiller), Germany.
- Cande, S. & Kent, D., 1995. Revised calibration of the geomagnetic polarity time scale, *J. geophys. Res.*, **100**(B4), 6093–6095.
- Cassignol, C. & Gillot, P.-Y., 1982. *Range and effectiveness of unspiked potassium-argon dating: Experimental groundwork and applications*, John Wiley, New York, pp. 159–179.
- Chernet, T., Hart W., Aronson, J. & Walter, R., 1998. New ages constraints on the timing of volcanism and tectonism in the northern Main Ethiopian Rift-southern Afar transition zone (Ethiopia), *J. Volc. Geotherm. Res.*, **80**, 267–280.
- Chessex, R., Delaloye, M., Muller, J. & Weidmann, M., 1975. Evolution of the volcanic region of Ali Sabieh (T. F. A. I.), in the light of K-Ar age determinations, in *Afar Depression of Ethiopia*, **1**, pp. 221–227, eds Pilger, A. & Roesler, A., E. Schweizer. Verlagsbuchhandl. (Naegle u. Obermiller), Stuttgart, Germany.
- Civetta, L., De Fino, M., Gasparini, P., Ghiara, M.R., La Volpe, L. & Lirer, L., 1975. Eastern Afar: Geology, Petrology, Geochemistry, in *Afar Depression of Ethiopia*, **1**, pp. 201–206, eds Pilger, A. & Roesler, A., E. Schweizer. Verlagsbuchhandl. (Naegle u. Obermiller), Germany.
- Cochran, J.R., 1981. The Gulf of Aden: structure and evolution of a young ocean basin and continental margin, *J. geophys. Res.*, **86**, 263–287.
- Cogné, J.P., 2003. Paleomac: a Macintosh application for treating paleomagnetic data and making plate reconstructions, *Geochem. Geophys. Geosyst.*, **4**(1), 1007.
- Coulié, E., 2001. Chronologie 40Ar/39Ar et K/Ar de la déchirure continentale en Afar depuis 30 Ma, PhD thesis, Université Paris Sud-Orsay, France.
- Coulié, E., Quidelleur, X., Gillot, P.-Y., Courtillot, V., Lefèvre, J.-C. & Chiesa, S., 2003. Comparative K-Ar and Ar/Ar dating of Ethiopian and Yemenite Oligocene volcanism: Implications for timing and duration of the Ethiopian Traps, *Earth planet. Sci. Lett.*, **206**, 477–492.
- Courtillot, V., 1980. Opening of the Gulf of Aden and Afar by progressive tearing, *Phys. Earth planet. Int.*, **21**, 343–350.
- Courtillot, V., Achache, J., Landre, F., Bonhommet, N., Montigny, R. & Féraud, G., 1984. Episodic spreading and rift propagation; new paleomagnetic and geochronologic data from the Afar nascent passive margin, *J. geophys. Res.*, **89**(5), 3315–3333.
- Courtillot, V., Armijo, R. & Tapponnier, P., 1987. Kinematics of the Sinai triple junction and a two-phase model of Arabia-Africa rifting, in *Continental Extensional Tectonics*, pp. 559–573, eds Coward, M.P., Dewey, J.F. & Hancock, P.L. Geol. Soc. London Spec. Publ., London.

- Courtillot, V., Jaupart, C., Manighetti, I., Tapponnier, P. & Besse, J., 1999. On causal links between flood basalts and continental breakup, *Earth planet. Sci. Lett.*, **166**, 177–199.
- Fisher, R.A., 1953. Dispersion on a sphere, *Proc. R. Soc. Lond., A*, **217**, 295–305.
- Galibert, P.Y., Sichler, B., Smith, B. & Bonhomme, N., 1980. Paléomagnétisme en zone d'accrétion: Le cas de l'Afar, *Bull. Soc. Geol. Fr.*, **22**, 881–890.
- Gasse, F. & Varet, J., 1986. Carte géologique de la République de Djibouti: feuille de Eali Sabieh, Ministère Français des Relations Extérieures et ISERST, 1/100000, Orstom, Djibouti.
- Gasse, F., Richard, O. & Fournier, M., 1987. Carte géologique de la République de Djibouti: feuille de Dikhil, Ministère Français des Relations Extérieures et ISERST, 1/100000, Orstom Djibouti.
- Gaulier, J.-M. & Huchon, P., 1991. Tectonic evolution of Afar triple junction, *Bull. Soc. Geol. Fr.*, **162**, 451–464.
- Gillot, P.-Y. & Cornette, Y., 1986. The Cassinot technique for potassium-argon dating, precision and accuracy: examples from late Pleistocene to recent volcanics from southern Italy, *Chem. Geol.*, **59**, 205–222.
- Gupta, A. & Scholz, C.H., 2000. A brittle strain regime transition in the Afar Depression: Implications for fault growth and seafloor spreading, *Geology*, **28**, 1087–1090.
- Halls, H.C., 1976. A least-squares method to find a remanence direction from converging remagnetization circles, *Geophys. J. R. astr. Soc.*, **45**, 297–304.
- Hess, J.C. & Lippolt, H.J., 1994. Compilation of K-Ar measurements on HD-B1 standard biotite, in *Phanerozoic Time Scale. Bull. Liais. Inform. I.U.G.S. Subcom. Geochronol. Vol. 12*, pp. 19–23, ed. Odin, G.S.
- Hilgen, F.J., 1991. Astronomical calibration of Gauss to Matuyama sapropels in the Mediterranean and implication for the geomagnetic polarity time scale, *Earth planet. Sci. Lett.*, **104**, 226–244.
- Hofmann, C., Courtillot, V., Feraud, G., Rochette, P., Yirgus, G., Ketefo, E. & Pik, R., 1997. Timing of the Ethiopian flood basalt event and implications for plume birth and global change, *Nature*, **389**, 838–841.
- Izzeldin, A.Y., 1987. Seismic, gravity and magnetic surveys in the central part of the Red Sea: their interpretations and implications for the structure and evolution of the Red Sea, *Tectonophysics*, **143**, 269–306.
- Kidane, T. *et al.*, 2003. New paleomagnetic and geochronologic results from Ethiopian Afar: Block rotations linked to rift overlap and propagation, and determination of a ~2 Ma reference pole for stable Africa, *J. geophys. Res.*, **108**, Art. No. 2102.
- Kirschvink, J.L., 1980. The least-squares line and plane and the analysis of palaeomagnetic data, *Geophys. J. R. astr. Soc.*, **62**, 699–718.
- Lahitte, P., 2000. Le volcanisme Plio-Quaternaire lié aux mécanismes d'ouverture de la dépression Afar, *PhD thesis*, Université Paris Sud-Orsay, France.
- Lahitte, P., Coulié, E., Mercier, N., Kidane, T. & Gillot, P.-Y., 2001. Chronologie K-Ar et TL du volcanisme aux extrémités sud du propagateur Mer Rouge en Afar depuis 300 ka, *Compte Rendu Acad. Sciences Paris*, **322**(1), 13–20.
- Lahitte, P., Gillot, P.-Y., Kidane, T., Courtillot, V. & Bekele, A., 2003. New age constraints on the timing of volcanism in central Afar, rifting emplacement implications, *J. geophys. Res.*, **108**, Art. No. 2123., *et al.*(2003) not cited in text.
- McDougall, I. & Harrison, T.M., 1988. *Geochronology and thermochronology by the <sup>40</sup>Ar/<sup>39</sup>Ar method*, Oxford Univ. Press, New York, pp. 212.
- McDougall, I., Brown, F.H., Cerling, T.E. & Hillhouse, J.W., 1992. A reappraisal of the geomagnetic polarity time scale to 4 Ma using data from the Turkana Basin, East Africa, *Geophys. Res. Lett.*, **19**, 2349–2532.
- McFadden, P.L. & Lowes, F.J., 1981. The discrimination of mean directions drawn from Fisher distributions, *Geophys. J. R. astr. Soc.*, **67**, 19–33.
- McFadden, P.L. & McElhinny, M.W., 1988. The combined analysis of remagnetization circles and direct observations in palaeomagnetism, *Earth planet. Sci. Lett.*, **87**, 161–172.
- Mahon, K.I., 1996. The New 'York' regression: application of an improved statistical method to geochemistry, *Int. Geol. Rev.*, **38**, 293–303.
- Manighetti, I., Tapponnier, P., Gillot, P.-Y., Jacques, E., Courtillot, V., Armijo, R., Ruegg, J.C. & King, G., 1998. Propagation of rifting along the Arabia Somalia plate boundary into Afar, *J. geophys. Res.*, **103**, 4347–4974.
- Manighetti, I., Tapponnier, P., Courtillot, V., Gallet, Y., Jacques, E. & Gillot, P.-Y., 2001. Strain transfer between disconnected, propagating rifts in Afar, *J. geophys. Res.*, **106**, 13 613–13 665.
- Muller, J. & Boucarut, M., 1975. Évolution structurale de la région d'Arta—Ali Sabieh (T.F.A.I.), Afrique Orientale, in *Afar depression of Ethiopia*, pp. 228–231, ed. Pilger, A., & Rösler, A., Schweizerbart, Stuttgart.
- Odin, G.S., 1982. *Numerical dating in stratigraphy* Wiley, Chichester, 1094.
- Quidelleur, X. & Courtillot, V., 1996. On low-degree spherical harmonic models of paleosecular variation, *Phys. Earth planet. Int.*, **95**, 55–77.
- Richard, O., 1979. Etude de la transition dorsale océanique-rift émergé: le golfe de Tadjoura (République de Djibouti), *PhD thesis*, Université de Paris Sud-Orsay, France.
- Rochette, P. *et al.*, 1998. Magnetostratigraphy and timing of the Oligocene Ethiopian traps, *Earth planet. Sci. Lett.*, **164**, 497–510.
- Ruegg, J.-C., Lepine, J.-C. & Tarantola, A., 1981. The Somalian Earthquakes of May, 1980, East Africa, *Geophys. Res. Lett.*, **8**, 817–820.
- Schult, A., 1974. Paleomagnetism of Tertiary volcanic rocks from the Ethiopian southern plateau and the Danakil block, *J. Geophys.*, **40**, 203–212.
- Sichler, B., 1980. La bielle danakile: Un modèle pour l'évolution géodynamique de l'Afar, *Bull. Soc. Geol. Fr.*, **6**, 925–933.
- Steiger, R.H. & Jäger, E., 1977. Subcommission on Geochronology: convention on the use of decay constants in Geo and Cosmochronology, *Earth planet. Sci. Lett.*, **36**, 359–362.
- Tamsett, D. & Searle, R., 1990. Structure of the Alula Fartak Fracture Zone, Gulf of Aden, *J. geophys. Res.*, **95**, 1239–1254.
- Tapponnier, P., Armijo, R., Manighetti, I. & Courtillot, V., 1990. Bookshelf faulting and horizontal block rotations between overlapping rifts in southern Afar, *Geophys. Res. Lett.*, **17**(1), 1–4.
- Taylor, J.R., 1982. *An introduction to error analysis* University Science Books, Mill Valley, pp. 270.
- Ukstins, I.A., Renne, P.R., Wolfenden, E., Baker, J., Ayalew, D. & Menzies, M., 2002. Matching conjugate volcanic rifted margins: 40Ar/39Ar chronostratigraphy of pre- and syn-rift bimodal flood volcanics in Ethiopia & Yemen, *Earth planet. Sci. Lett.*, **198**, 283–306.
- Varet, J. & Gasse, F., 1978. Carte géologique de l'Afar central et méridional (Ethiopie et T.F.A.I.) au 1/500 000, C.N.R.S.-C.N.R., Geotechnip. La Celle Saint-Cloud.
- WoldeGabriel, G., Haile-Selassie, Y., Renne, P., Hart, W., Ambrose, S., Asfaw, B., Heiken, G. & White T., 2001. Geology and palaeontology of the Late Miocene Middle Awash valley, Afar rift, Ethiopia, *Nature*, **412**, 175–177.
- Zijderveld, J.D.A., 1967. A.C. demagnetization of rocks—analysis of results, in *Methods in Paleomagnetism*, pp. 254–286, eds Collinson, D.W., Creer, K.M. & Runcorn, S.K., Elsevier, New York.
- Zumbo, V., Feraud, G., Vellutini, P., Pignat, P. & Vincent, J., 1995. First 40Ar/39Ar dating on Early Pliocene to Plio-Pleistocene magmatic events of the Afar—Republic of Djibouti, *J. Volc. Geotherm. Res.*, **65**, 281–295.